High Intensity RF Linear Accelerators

2.3 Emittance Growth and Halo Formation in Focusing Channels

Yuri Batygin

Los Alamos National Laboratory

U.S. Particle Accelerator School

Albuquerque, New Mexico, 23 – 27 June 2014

Content

Definition and Outcome of Beam Halo

Beam Losses and Residual Activation along LANSCE Linac

Sources of Emittance Growth and Halo Formation in Linacs

Effect of Spherical Aberration on Beam Emittance

Effect of Space Charge Aberration on Beam Emittance

Beam Uniforming

Beam Emittance Growth in a Focusing Channel

Halo Development in Particle-Core Interaction

LANL Beam Halo Experiment

Experimental Observation of Space-Charge Driven Resonances in
 Linac

Proposed FODO Quadrupole - Duodecapole Channel for Suppression
 of Halo Formation

Linac Beam Intensity Distribution in Phase Space
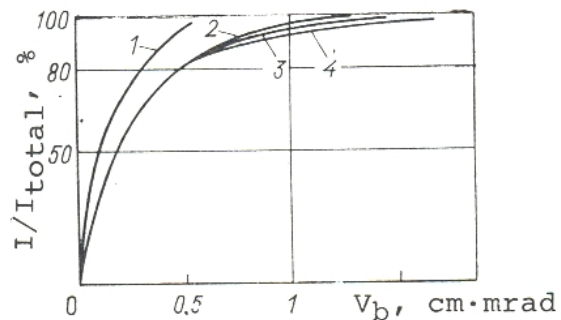
Fig. 4.8   The distribution of the current in the phase space of the beam at different points in the CERN proton accelerator-injector.   1--0.5 MeV, 115 mA; 2--10 MeV; 3--30 MeV; 4--50 MeV, 58 mA.
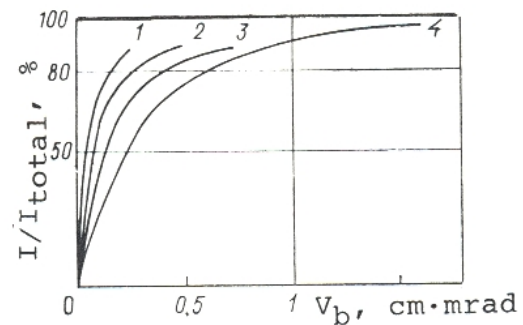
Fig. 4.9   The distribution of the current in the phase space of the beam in the FNAL proton accelerator-injector.   1--0.75 MeV, 150 ma; 2--10 MeV; 3 and 4--200 MeV, 78 mA.

Definition and Outcome of Beam Halo

1. Beam halo - a collection of particles which lies outside of beam core and typically contain small fraction of the beam (less than 1%).

2. Beam halo is a main source of beam losses which results in radio-activation and degradation of accelerator components.

3. Modern accelerator projects using high-intensity beams with final energies of 1-1.5 GeV and peak beam currents of 30-100 mA require keeping the beam losses at the level of 10^{-7}/m (less than 1 Watt/m) to avoid activation of the accelerator and allowing hands-on maintenance over long operating periods.

4. Collimation of beam halo cannot prevent beam losses completely, because the halo of a mismatched beam re-develops in phase space after a certain distance following collimation.
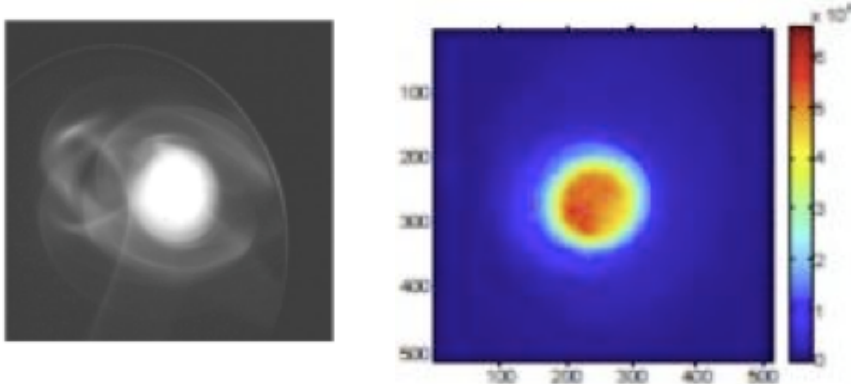
Beam halo monitoring at Liverpool University

http://liv.ac.uk/quasar/research/beam-instrumentation/beam-halo-studies/

The LANSCE accelerator provides unique flexible time-structured beams from 100 to 800 MeV

Ultra Cold Neutron (UCN) Area

RLW plant

Area A (Future MTS)

Proton Radiography (pRad)

Lujan Center
1L Target

Cooling Towers

WNR
Target 4
Target 2

Side-coupled-cavity accelerator and equipment building (100-800 MeV)

Central Control Room

Isotope Production Facility

Drift tube accelerator and equipment building (0.75-100 MeV)

Injector (0-0.75 MeV)

Los Alamos
NATIONAL LABORATORY
EST.1943

Operated by the Los Alamos National Security, LLC for the DOE/NNSA

5

NNSA

LANSCE Facility Overview

H+ Source

H- Source

Isotope Production Facility

Proton Radiography

Ultra-Cold Neutrons

Drift Tube Linac

Coupled-Cavity Linac

Area A (inactive - future home of MTS)

- 750 keV H+ and H- Injectors
- 100 MeV Drift Tube Linac (4 tanks)
- 800 MeV Coupled Cavity Linac (44 modules)
- 800 MeV Compressor Ring (PSR)

PSR

Lujan Center

ER-1

Target 1
Target 2

9
10 11A/B
12
13
14
15
16
1
2
ER-2

7
6
8
4 3
120L

90R
5
60R
30R
15R
15L 30L
90L

Target 4

Weapons Neutron Research Facility

○ kicker
◆ chopper

LANSCE Accelerating Structures

H+ Source

0.75 MeV

H- Source

Drift Tube Linear Accelerator

Transition Region

100 MeV

Side-Coupled Linear Accelerator

800 MeV

MODULE 27

Beam Losses and Residual Activation along LANSCE Linac

- Typical Lujan Operation, I_{avg}=110 uA , DF=1.25%, chop=290ns/358ns

- Linac loss monitors - liquid scintillator & PMT (integrating (shown here) and instantaneous modes)

cal'd against 100 nA point spill

Transv & long losses in 100 MeV matching region

Long & transv losses in lattice transition

Loss Monitor - % of Threshold

Snapshot on Aug 20, 2010

Drift Tube Linac

800 MeV Coupled-Cavity Linac

H- Source

$\Delta I_{cm} < 0.2\%$

$\Delta I_{cm} < 0.1\%$
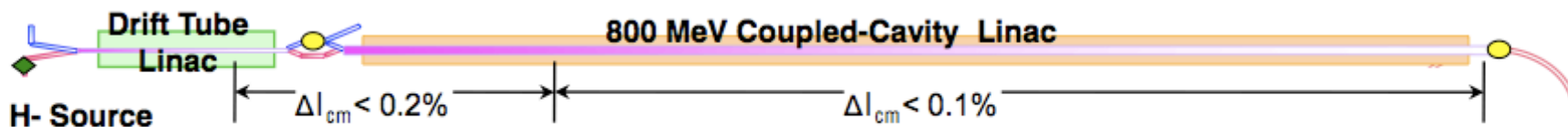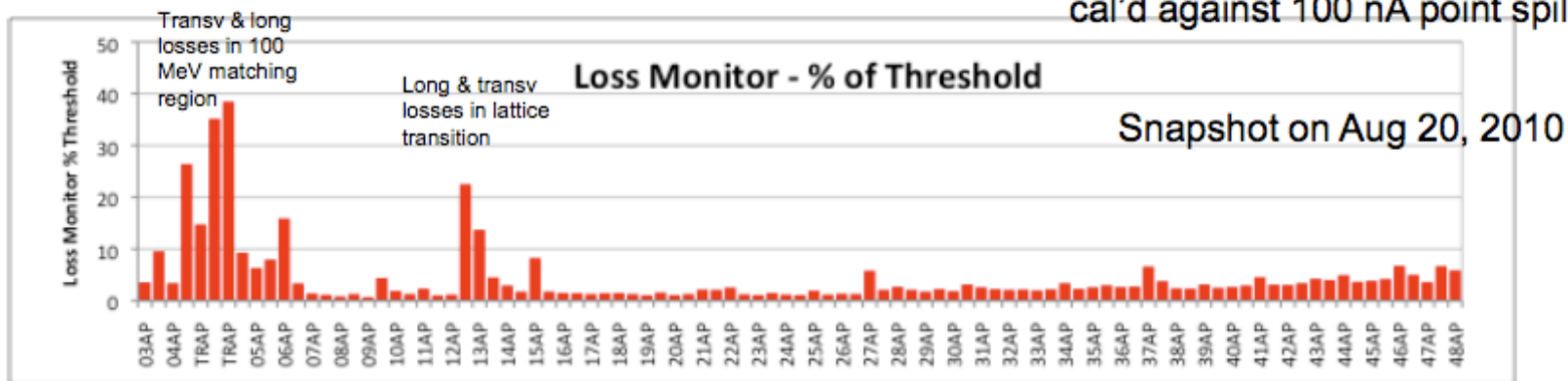
Linac Activation Levels (mR/hr @ 30 cm)

Typ. 1-10; Max. < 90

Isolate spots ~ few 10's

Activation Survey @ 30 cm on July 17, 2010 (~ beam off + 16 hours)

Los Alamos

8

Beam Loss Monitors

Scintillation based detector

Gamma detector: ion chamber based loss monitor

LANSCE beam spill monitoring along high-energy beamlines
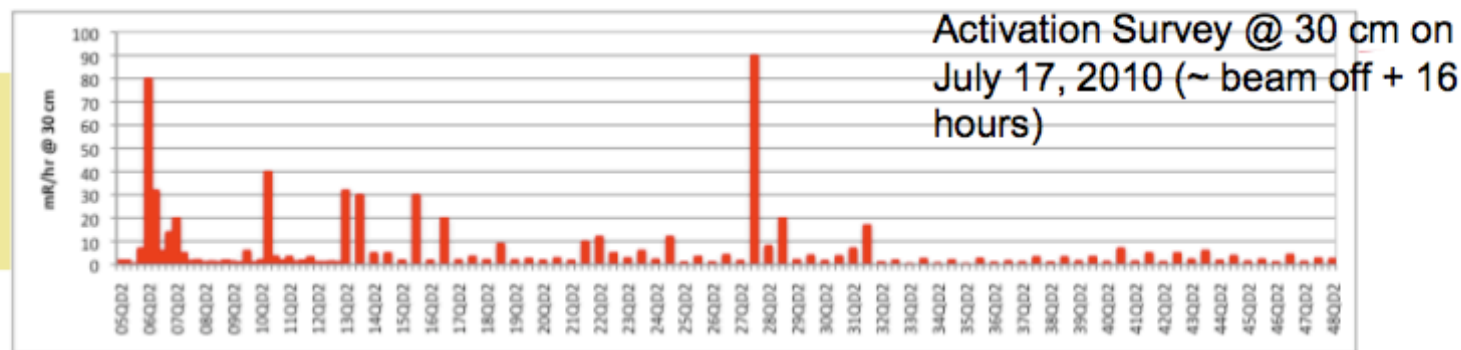
Sources of Emittance Growth and Halo Formation in Linacs

1. Mismatch of the beam with focusing and accelerating structures

2. Transverse-longitudinal coupling in RF field

3. Misalignments of accelerator channel components

4. Aberrations and nonlinearities of focusing elements

5. Beam energy tails from un-captured particles

6. Particle scattering on residual gas and intra-beam scattering

7. Non-linear space-charge forces of the beam: filamentation, resonances

Spherical aberrations

So far we analyzed space charge dominated beam transport in linear approximation to space charge forces. In the presence of linear focusing field, the beam emittance remains constant. Realistic focusing elements posses strong aberrations, which result in distortion of phase space area, occupied by the beam. Among others, the spherical aberration cannot be eliminated, and therefore, has the most significant effect on particle dynamics.
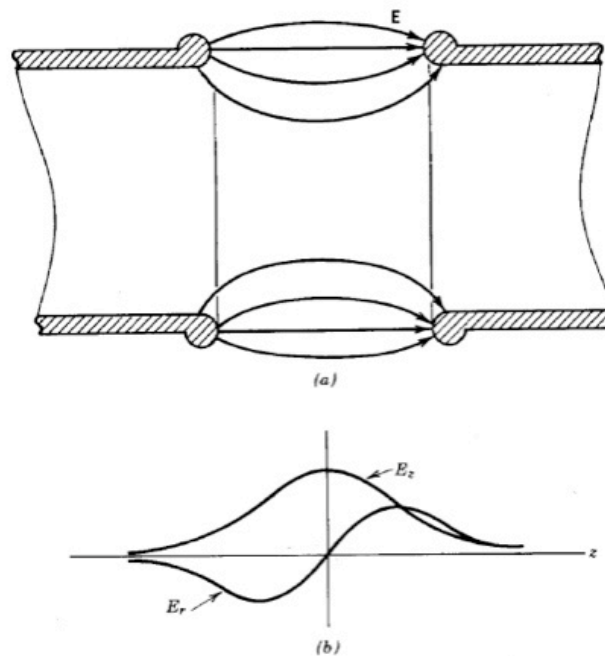
Field distribution in electrostatic lens gap.

Potential of Axial-Symmetric Lens

Potential of axial-symmetric electrostatic lens is defined by Laplace's equation:

$$\frac{1}{r}\frac{\partial}{\partial r}(r\frac{\partial U}{\partial r})+\frac{\partial^2 U}{\partial z^2}=0 \qquad (3.1)$$

Solution:
$$U(z,r)=U(z)-\frac{r^2}{4}U''(z)+\frac{r^4}{64}U^{(4)}(z)-\frac{r^6}{2304}U^{(6)}(z)+... \qquad (3.2)$$

Field distribution inside each gap is given by near-axis approximation:

$$E_z(r,z)=E_z(z)-\frac{r^2}{4}E_z^{(2)}(z)+\frac{r^4}{64}E_z^{(4)}(z)+.....+\frac{(-1)^n E_z^{(2n)}}{(n!)}(\frac{r}{2})^{2n}, \qquad (3.3)$$

$$E_r(r,z)= -\frac{r}{2}E_z'(z)+\frac{r^3}{16}E_z^{(3)}(z)....+\frac{(-1)^n E_z^{(2n-1)}}{(n!)(n-1)!}(\frac{r}{2})^{2n-1}. \qquad (3.4)$$

Equation of particle motion

$$\frac{d^2x}{dz^2} = \frac{q}{mv_z^2} x \left(-\frac{1}{2}\frac{\partial E_z}{\partial z} + \frac{r^2}{16}\frac{\partial^3 E_z}{\partial z^3} + ...\right)$$

Let us neglect the change of particle position in x - direction while crossing the gap. Change of slope of particle trajectory at the entrance of the first gap is

$$\Delta(\frac{dx}{dz})_{in} = \frac{1}{v_{in}^2}\frac{q}{m} x \left(-\frac{1}{2}\int_{-\infty}^{d/2} \frac{dE_z}{dz} dz + \frac{r^2}{16}\int_{-\infty}^{d/2} \frac{d^3 E_z}{dz^3} dz\right) = -\frac{q}{m}\frac{E_z}{2 v_{in}^2} x \; (1 - \frac{r^2}{8 E_z}\frac{d^2 E_z}{dz^2})$$

where v_{in} is an effective particle velocity at the entrances of the gap, and the values of the field are taken at the center of the gap. Analogously, the change of the slope of the particle trajectory at the exit of the first gap is

$$\Delta(\frac{dx}{dz})_{out} = \frac{q}{m}\frac{E_z}{2 v_{out}^2} x \; (1 - \frac{r^2}{8 E_z}\frac{d^2 E_z}{dz^2})$$

where v_{out} is an effective particle velocity at the exit of the first gap. Total change of slope of the particle at the first gap is

$$\Delta(\frac{dx}{dz}) = \frac{q}{mc^2}\frac{E_z}{2} x \; (\frac{1}{\beta_{out}^2} - \frac{1}{\beta_{in}^2}) (1 - \frac{r^2}{8 E_z}\frac{d^2 E_z}{dz^2})$$

13

To calculate term in brackets, let us approximate the field in the gap by function $E_z = \dfrac{E_o}{1 + (\frac{z}{L})^2}$

where L is a half of an effective gap width $L \approx \dfrac{d + a}{2}$

The second derivative $\dfrac{d^2 E_z}{dz^2} = -\dfrac{2E_o}{L^2} \dfrac{[1 - 3(\frac{z}{L})^2]}{[1 + (\frac{z}{L})^2]^3}$
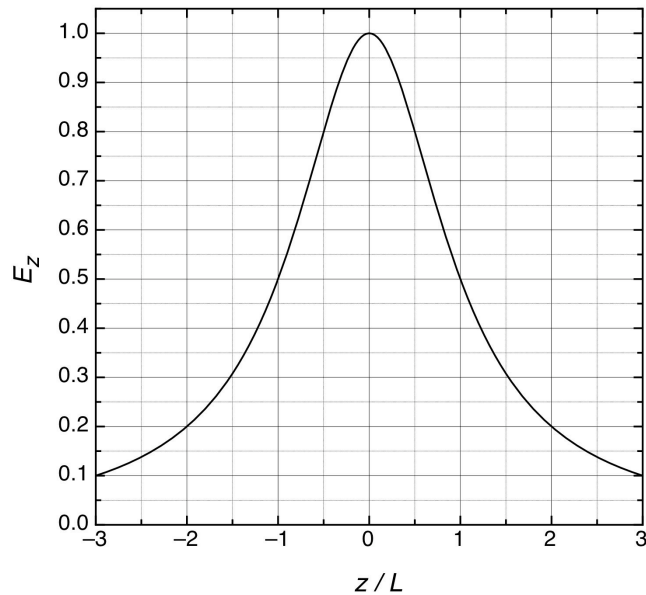
Approximation of the static field in the gap.

The term in bracket taken at the center of the gap:

$$1 - \frac{r^2}{8E_z}\frac{d^2E_z}{dz^2} = 1 + \frac{r^2}{4L^2}$$

Finally, the change of slope of particle trajectory at the gap is

$$\Delta(\frac{dx}{dz}) = \frac{q}{mc^2}\frac{E_z}{2}x(\frac{1}{\beta_{out}^2} - \frac{1}{\beta_{in}^2})(1 + \frac{r^2}{4L^2})$$

If the field in the gap accelerates particles, $E_z > 0$, then $\beta_{out} > \beta_{in}$, and change of slope of particle trajectory is negative $\Delta(\frac{dx}{dz}) < 0$

If the field in the gap decelerates particles, $E_z < 0$, then $\beta_{out} < \beta_{in}$, and change of slope of particle trajectory is also negative $\Delta(\frac{dx}{dz}) < 0$

The *gap with electrostatic field focuses particles*. Change of slope of particle trajectory can be written via focal length f and aberration coefficient C_a:

$$\Delta(\frac{dx}{dz}) = -\frac{x}{f}[1 + C_\alpha r^2] \qquad C_\alpha = \frac{1}{(2L)^2}$$

15
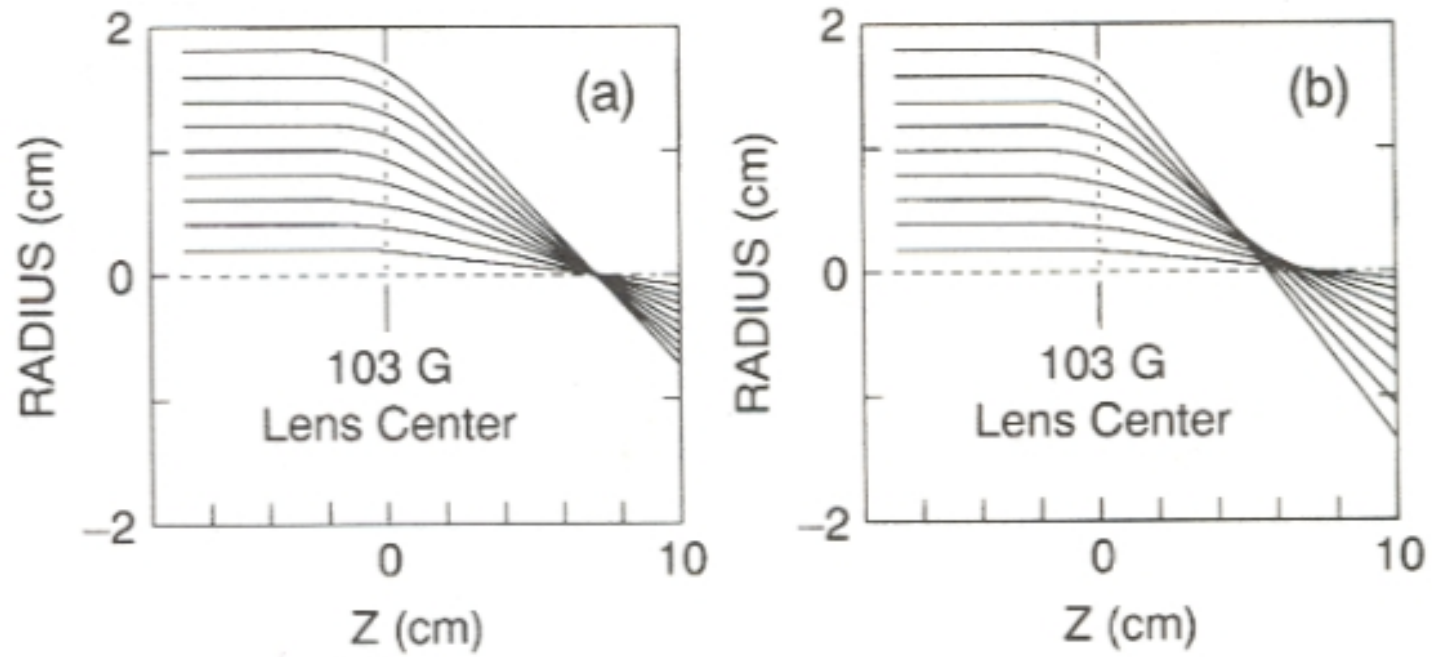
Focusing of a parallel beam by (a) an ideal lens (a) and
(b) by lens with spherical aberrations (from Reiser, 1994, p. 458).

Scherzer Theorem (1936)

Spherical aberrations are unavoidable if

- the lens fields are rotationally symmetric
- the electromagnetic fields are static
- there are no space charges
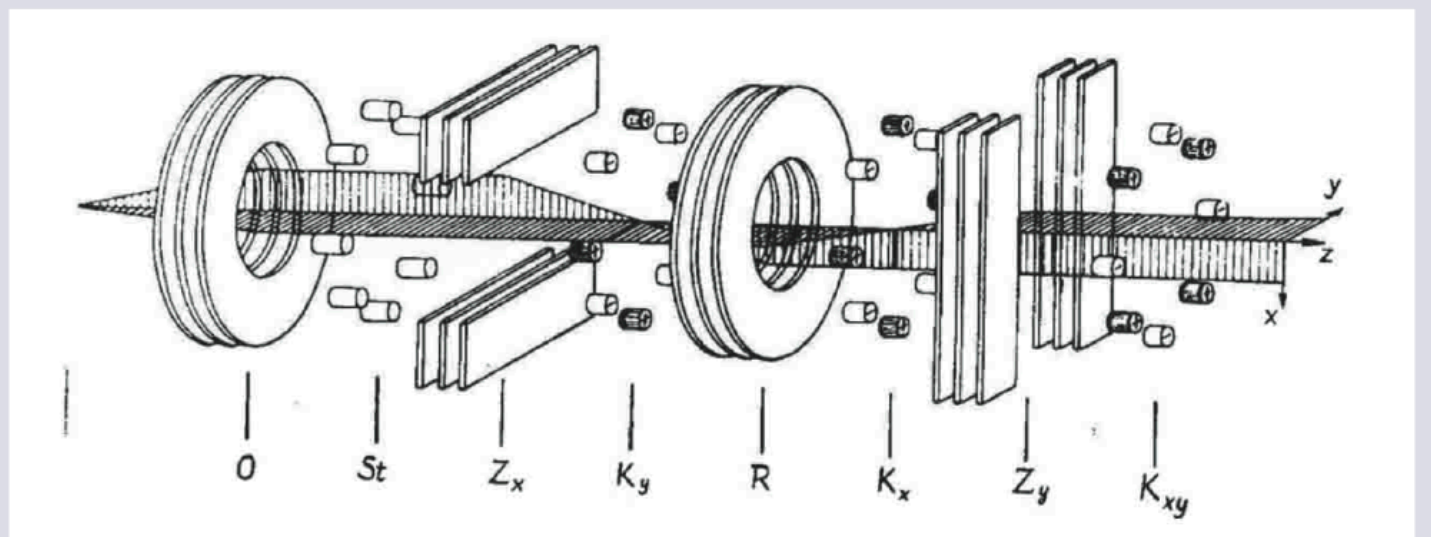
Fig. 7. The Scherzer corrector, as constructed in the 1950s (from Seeliger, 1951): Objective lens (O), stigmator (St), electrostatic cylinder lenses (Z), round lens (R), octopoles (K).

Beam Emittance Growth due to Spherical Aberrations

Initial beam distribution:

$$\frac{x_o^2}{R^2}\varepsilon + \frac{x_o^{'2}}{\varepsilon}R^2 = \varepsilon$$

Transformation through the lens

$$x = x_o$$
$$x' = x_o' - (1 + \frac{C_s}{f^3}r_o^2)\frac{x_o}{f}$$

Change variables (x, x') to action-angle variables (J, ψ)

$$\frac{x}{R}\sqrt{\mathfrak{z}} = \sqrt{2J}\,\cos\psi$$
$$(x' + \frac{x}{f})\frac{R}{\sqrt{\mathfrak{z}}} = \sqrt{2J}\,\sin\psi$$

Beam ellipse distortion:

$$T + T^2 2\upsilon\sin\psi\cos^3\psi + T^3\upsilon^2\cos^6\psi = 1$$

where

$$T = \frac{2J}{\varepsilon} \qquad \upsilon = \frac{C_s R^4}{\mathfrak{z}\,f^4}$$

Distortion of beam emittance due to space charge aberration
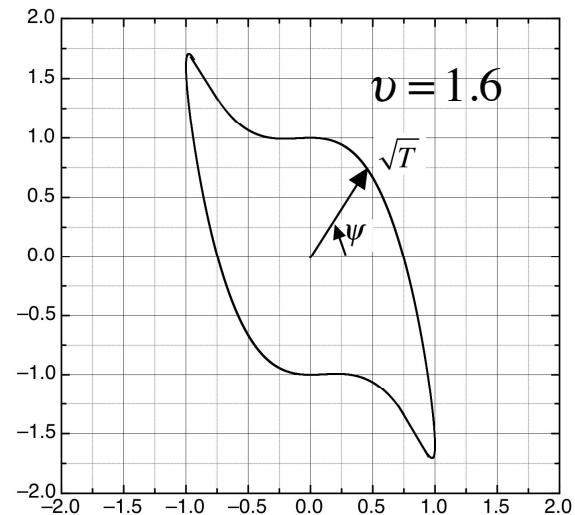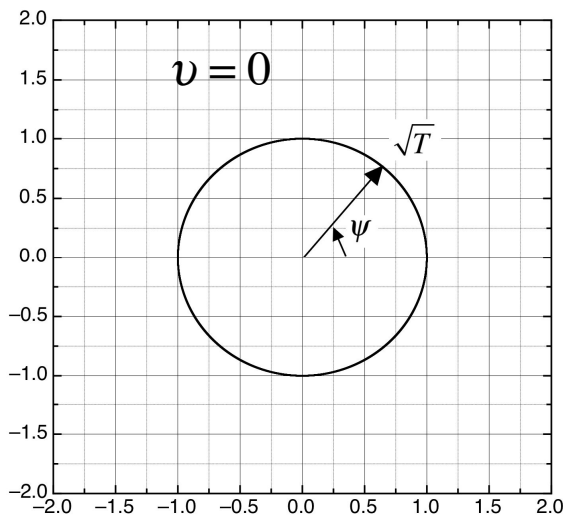
In general case, arbitrary transformation

$$x = x_o , \qquad\qquad x' = x_o' + f(x_o, y_o) , \qquad\qquad (3.20)$$

conserves phase space area due to Jacobian of transformation (3.20) always equals unity:

$$\begin{vmatrix} \dfrac{\partial x}{\partial x_O} & \dfrac{\partial x}{\partial x_o'} \\[2ex] \dfrac{\partial x'}{\partial x_O} & \dfrac{\partial x'}{\partial x_O'} \end{vmatrix} = 1 \qquad\qquad (3.21)$$

While phase space areas occupied by the beam before and after lens are the same, the effective area, occupied by the beam, is increased. The value of beam emittance can be estimated as a total area of elements *dx dx'* occupied by the beam. Actual areas of the beam in both cases are the same, but the number of elements covered by the beam at phase pane is different.

Let us denote the increase of effective beam emittance as a square of product of minimum and maximum values of T:

$$\frac{\Im_{eff}}{\Im} = \sqrt{T_{max}\, T_{min}} \; . \tag{3.22}$$

Values T_{max}, T_{min} are determined numerically. Dependence of emittance growth versus parameter υ is presented at figure below. Dependence can be approximated by the function:

$$\frac{\Im_{eff}}{\Im} = \sqrt{1 + K\upsilon^2}, \qquad \upsilon = \frac{C_\alpha R^4}{f\,\Im} \tag{3.23}$$

where parameter $K \approx 0.4$. Finally, effective beam emittance growth due to spherical aberrations:
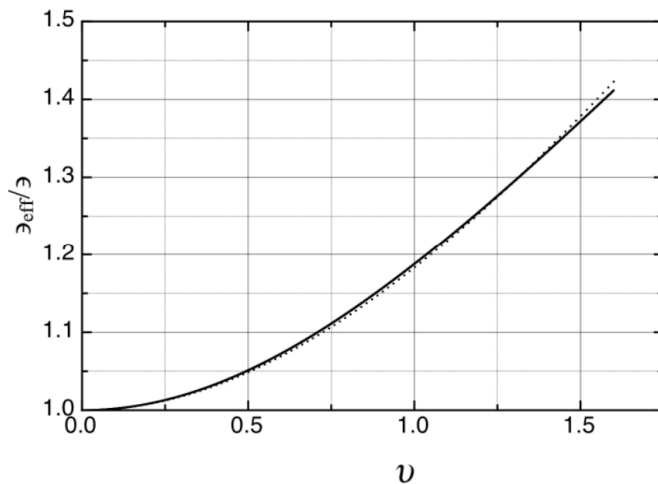
$$\frac{\Im_{eff}}{\Im} = \sqrt{1 + K(\frac{C_\alpha R^4}{f\,\Im})^2} \tag{3.24}$$

Beam emittance growth after beam passing through axial-symmetric lens as a function of parameter υ : (sold line) Eq. (3.22), (dotted line) approximation by Eq.(3.23).

Emittance Growth due to Spherical Aberrations in Round Beam

KV

Water Bag

Parabolic

Gaussian
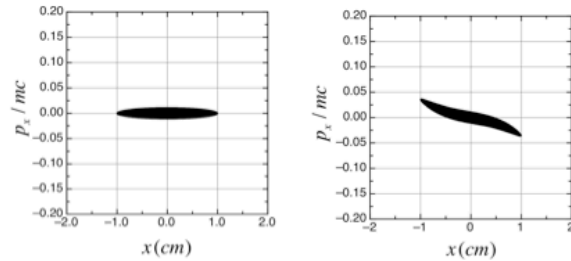
Expression for beam emittanc growth due to spherical aberrations

$$\frac{\ni_{eff}}{\ni} = \sqrt{1 + K(\frac{C_\alpha R^4}{f\,\ni})^2}$$

was tested numerically for round beam with different particle distributions. As a measure of effective beam emitance, the four-rms beam emittance was used and 2-rms beam size was used as a measure of beam radius:

$$\ni = 4\sqrt{<x^2><x'^2> - <xx'>^2} \qquad R = 2\sqrt{<x^2>}$$

Simulations confirm, that dependence is valid for round beam as well, while coefficient K depends on beam distribution (see Table). Value of coefficient K is mostly smaller than that determined above, except that for Gaussian distribution.
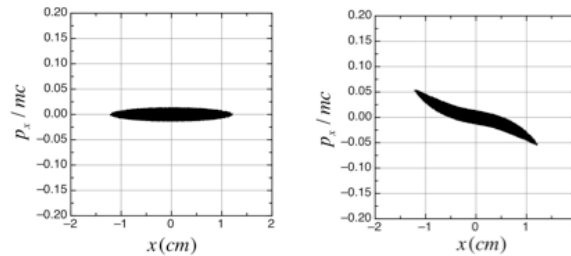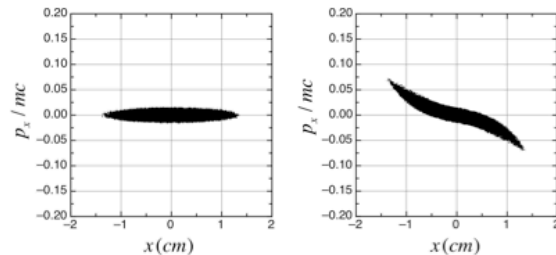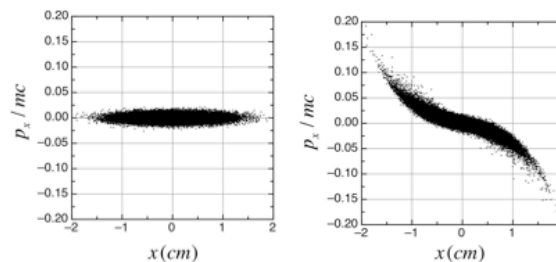
Distribution	Coeff. K
KV	0.0556
Water Bag	0.114
Parabolic	0.164
Gaussian	0.541

21

Redistribution of Beam Intensity due to Spherical Aberrations

Consider beam of particles parallel to the axis, entering lens. Particle radius after lens is given by:

$$r = r_o[1 - \frac{z}{f}(1 + C_\alpha r_o^2)]$$

where z is a drift distance from the lens. To find the beam density redistribution, let us take into account that the number of particles dN inside a thin ring $(r, r + dr)$ is kept constant during the drift of the beam at certain distance unless particle trajectories cross each other. Hence, the particle density $\rho(r) = dN/(2\pi r dr)$ at any z is connected with the initial density $\rho(r_o)$ by the equation $\rho(r)\,dr^2 = \rho(r_o)\,dr_o^2$, or:

$$\rho(r) = \frac{\rho(r_o)}{[1 - \tau(1 + C_\alpha r_o^2)]^2 + \eta^2 - 2r_o^2 \tau C_\alpha [1 - \tau(1 + C_\alpha r_o^2)]}$$

where $\tau = z/f$.
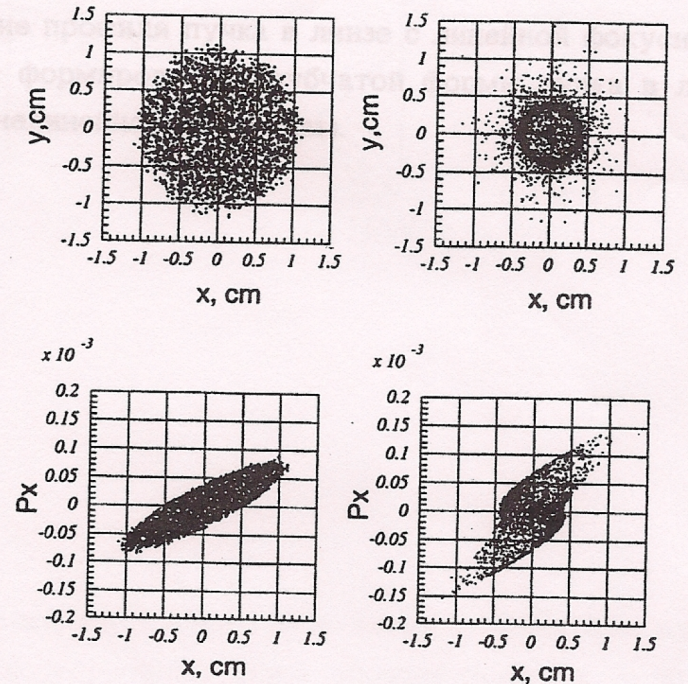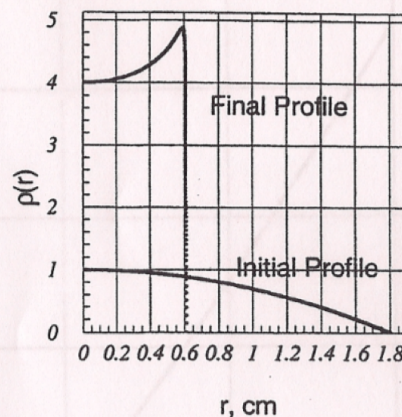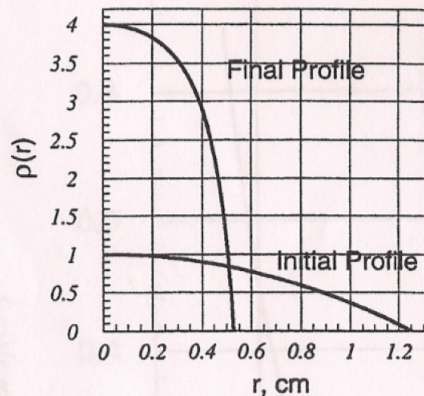
Beam cross sections and phase space distribution before and after crossing the lens with strong nonlinear field

(Left) conservation of beam profile in a lens with linear focusing, and (right) hollow beam formation on a lens with strong nonlinear field.

22

Reduction of Effect of Spherical Aberration in Einzel Lens

Focal length:

$$\frac{1}{f} = \frac{3}{8d}\left(\frac{\chi^2}{1+\chi}\right)$$

Ratio of potential difference of the lens U to particle energy W

$$\chi = U / W$$

Aberration coefficient ($K = 4\ldots30$)

$$C_\alpha = \frac{K}{R^2}$$
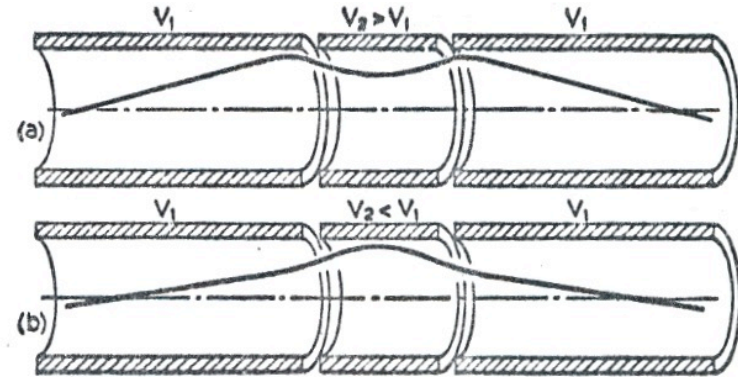
FIG. 6.2—A short cylinder between two cylinders at a different potential forms a converging lens whether the short cylinder is lower or higher in potential than the outer

In accelerating gap particles are focusing at the entrance of the lens. Therefore, in lens with accelerating voltage increment of paticles radius is negative $dr < 0$, while in lens with decelerating voltage $dr > 0$.
Coefficient of spherical aberration has to be corrected taking into account increment of particle radius inside the gap

$$\Delta r_{aberration} = C_\alpha r^3 = C_\alpha(\bar{r}+dr)^3 \approx C_\alpha \bar{r}^3(1+3\frac{dr}{\bar{r}})$$

$$\bar{C}_\alpha = C_\alpha(1+3\frac{dr}{\bar{r}})$$

Aberration is stronger in decelerating lens than in accelerating lens at the same value of the focal length.

23

Effect of Space Charge Aberration on Beam Emittance

Space charge density and space charge field of the beam with Gaussian distribution are given by
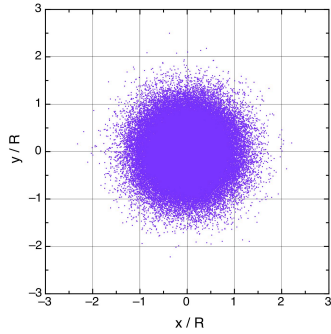
$$\rho(r_o) = \frac{2I}{\pi R_o^2 \beta c} \; exp(-2\frac{r_o^2}{R_o^2})$$

$$E_b = \frac{I}{2\pi \varepsilon_o \beta c} \frac{1}{r_o} [\,1 - exp(-2\frac{r_o^2}{R_o^2})\,]$$
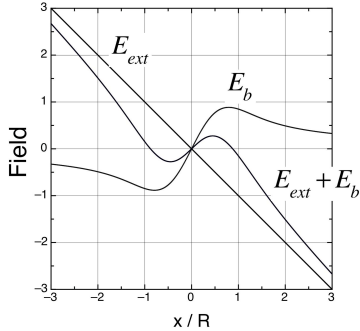
Nonlinear function in space charge field is expanded as

$$f(r_o) = 1 - exp(-2\frac{r_o^2}{R_o^2}) \approx 2\frac{r_o^2}{R_o^2} - 2\frac{r_o^4}{R_o^4} + \ldots$$

At the initial stage of beam emittance growth we can assume, that particle radius is unchanged, while the slope of the trajectory is changed. It gives us the nonlinear transformation:

$$r = r_o$$

$$r' = r_o' + \frac{2zP^2}{R_o^2}r_o - \frac{2zP^2}{R_o^4}r_o^3$$

where $P^2 = \dfrac{2I}{I_c \beta^3 \gamma^3}$ is the generalized perveance, $I_c = 4\pi\varepsilon_o mc^3/q$ is the characteristic beam current.

24

KV

Water Bag

Parabolic

Gaussian
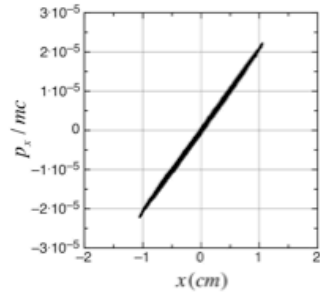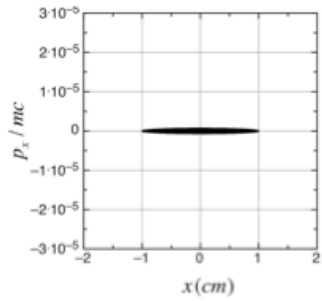
Parameter υ, which determines effect of spherical abberation on beam emittance is

$$\frac{C_\alpha R_o^4}{f\Im} = \frac{4}{\beta^3\gamma^3}\frac{I}{I_c}\frac{z}{\Im}$$
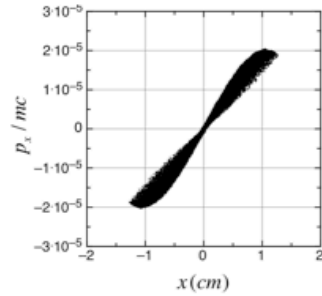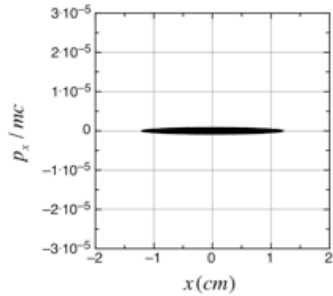
Therefore, space charge induced beam emittance growth in free space is:

$$\frac{\Im_{eff}}{\Im} = \sqrt{1 + \bar{K}(\frac{I}{I_c\beta^3\gamma^3}\frac{z}{\Im})^2}$$
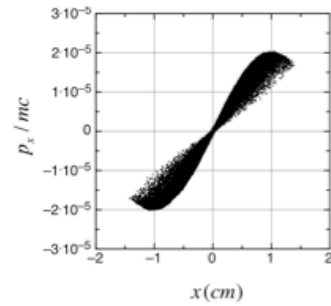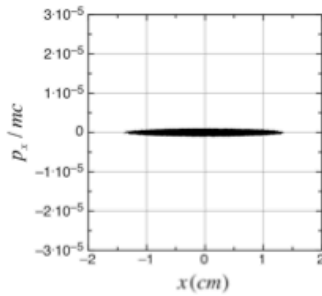
Parameter $\bar{K}$ was determined numerically for different distributins. Results are summarized in Table. As follows from above equation, initial emittance growth does not depend on initial beam radius.
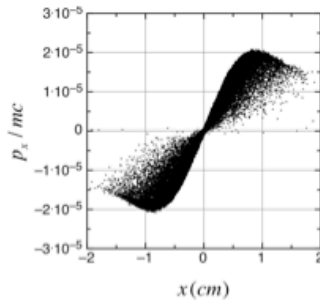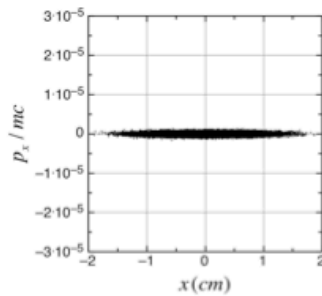
Distribution	Coeff. $\bar{K}$
KV	0
Water Bag	0.094
Parabolic	0.187
Gaussian	0.55

25

Experimental Observation of Effect of Nonlinear Space Charge Forces on Beam Emittance
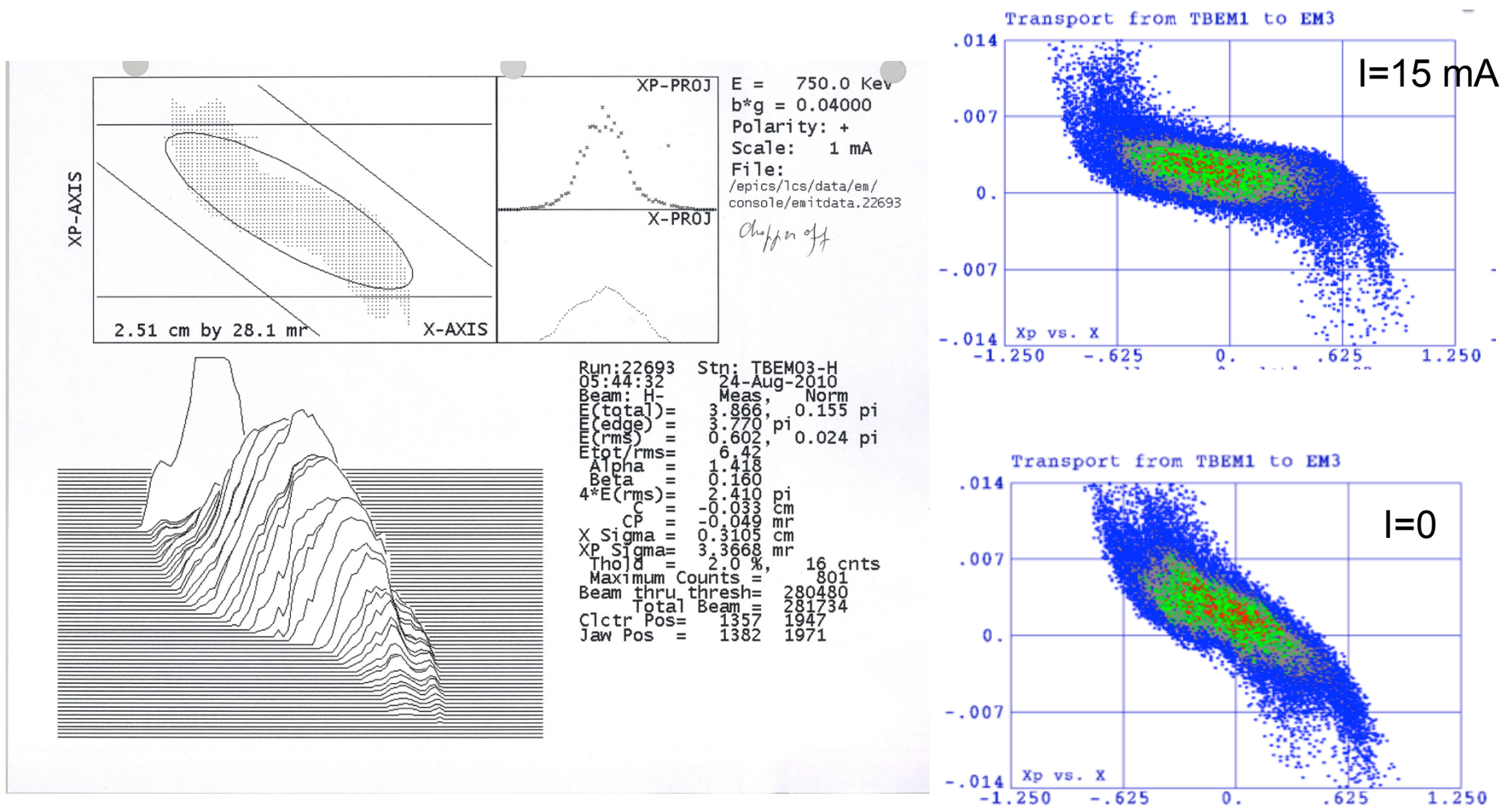
(Y.B. et al, Proc. of PAC2011, p. 64)

Suppose that the density is parabolic, given by

$$n(x,y) = \frac{2N_1}{\pi ab}\left[1 - \frac{x^2}{a^2} - \frac{y^2}{b^2}\right],$$

within the boundary of the ellipse defined by

$$\frac{x^2}{a^2} + \frac{y^2}{b^2} = 1.$$

Figure 3. Effect of space charge from a parabolic density on an initial zero-emittance beam. The initial and final phase-space distributions are shown.

$$\varepsilon_x = KL\frac{a}{b}\sqrt{\frac{1}{432}\frac{\left(\frac{2a}{b}+1\right)^2}{\left\{1+\frac{a}{b}\right\}^4} + \frac{7}{720}\frac{1}{\left\{1+\frac{a}{b}\right\}^4} - \frac{1}{360}\frac{\left(\frac{2a}{b}+1\right)}{\left\{1+\frac{a}{b}\right\}^4}}.$$

Figure 4. Final rms emittance values versus ellipse-aspect ratio a/b for a beam with parabolic density.

Beam Uniforming in Drift Space

Space charge forces of Gaussian beam are nonlinear function of radius which result in nonlinear redistribution of space charge density. At the beam drift, there is a certain distance where different layers of the beam do not cross each other: the radial motion of the particles is nonlinear, but the beam flow is still laminar. The assumption of laminar flow holds as long as $p_x(x)$ remains single-valued function. For laminar flow, the number of particles contained in an arbitrary cylinder with initial radius r_o remains constant. Use of Gauss theorem yields the result:

$$E_r r = E_{r_o} r_o = \frac{1}{\varepsilon_o} \int_0^{r_0} \rho(r^{'}) r^{'} \, dr^{'} = const \, .$$

(3.32)

Here, r is the radius of our hypothetical cylinder, which expands as the beam drift, thus $r = r(z)$, $r(z=0)=r_o$. Use of Eq. (3.32) yields the radial space charge force at any location:

$$E_r = \frac{I}{2 \pi \varepsilon_o \beta c} \frac{f(r_o)}{r} \, ,$$

(3.33)

$$f(r_o) = [1 - exp(-2\frac{r_o^2}{R_o^2})] \, .$$

(3.34)

Taking into account expression for space charge field, Eq. (3.33), the equation of motion of an arbitrary particle in drift region $dp_r / dt = qE_r / \gamma^2$ under the self space charge forces has the form:

$$\frac{d^2 r}{dz^2} = \frac{2I}{I_c \beta^3 \gamma^3} \frac{f(r_o)}{r} .$$ (3.35)

Let us introduce the new variables:

$$\bar{R} = \frac{r}{r_o} , \qquad Z = \frac{z}{r_o} \sqrt{\frac{4 I f(r_o)}{I_c \beta^3 \gamma^3}} ,$$ (3.36)

Then the Eq. (3.35) becomes:

$$\frac{d^2 \bar{R}}{dZ^2} = \frac{1}{2\bar{R}}$$ (3.37)

Eq. (3.37) is an equation for a single particle within the beam. It coinsides with envelope equation for the beam with negligible emittance. The first integral of the equation (3.37) is:

$$(\frac{d\bar{R}}{dZ})^2 - (\frac{d\bar{R}}{dZ})_o^2 = \ln \bar{R} .$$ (3.38)

The approximate solution of this equation is $\bar{R}(Z) = 1 + 0.25 Z^2 - 0.017 Z^3$. It gives for evolution of particle radius in drift space:

$$r = r_o [1 + \frac{1}{4} \eta (\frac{R_o}{r_o})^2 f(r_o) - 0.017 \eta^{3/2} (\frac{R_o}{r_o})^3 f^{3/2}(r_o)] ,$$ (3.39)

$$\eta = \frac{4I}{I_o \beta^3 \gamma^3} \frac{z^2}{R_o^2} ,$$ (3.40)

29

Let us take into account that the number of particles *dN* inside a thin ring (*r, r + dr*) is constant during the drift of the beam at certain distance, hence the particle density $\rho(r)=dN/(2\pi r dr)$ at any *z* is connected with the initial density $\rho(r_o)$ by the equation:

$$\rho(r) = \rho(r_o)\, \frac{r_o\, d\, r_o}{r\, d\, r}\,.$$

(3.41)

Calculation of derivatives (3.41) gives the redistribution of the Gaussian beam under self space charge forces :

$$\rho(r) = \frac{\rho_o\, exp\,(-2\xi_o^2)}{a_o + a_1 F + a_2 F^2 + a_3 F^3 + a_4 F^4 + a_5 F^5 + a_6 F^6}\,,$$

(3.42)

η=0

η=3.8

30
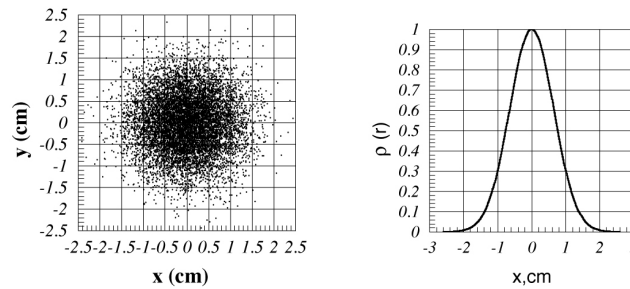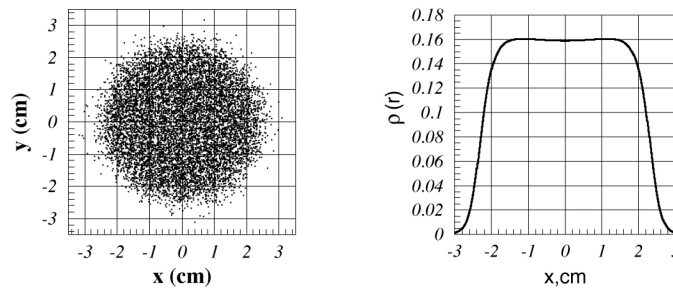
Fig. 3.6. Redistribution of Gaussian beam in drift space.

In Eq. (3.42) the following notations are used:

$$\xi_o = \frac{r_o}{R_o},$$

(3.43)

$$F = \sqrt{\frac{1 - exp(-2\xi_o^2)}{\xi_o^2}},$$

(3.44)

$$a_o = 1 + \eta \, exp(-2\xi_o^2),$$

(3.45)

$$a_1 = -0.102 \, \eta^{3/2} \, exp(-2\xi_o^2),$$

(3.46)

$$a_2 = \frac{1}{4} \eta^2 \, exp(-2\xi_o^2),$$

(3.47)

$$a_3 = 0.017 \, \eta^{3/2} - 0.0425 \, \eta^{5/2} \, exp(-2\xi_o^2)$$

(3.48)

$$a_4 = 1.734 \cdot 10^{-3} \, \eta^3 exp(-2\xi_o^2) - \frac{1}{16} \eta^2,$$

(3.49)

$$a_5 = 0.01275 \, \eta^{5/2},$$

(3.50)

$$a_6 = -5.78 \cdot 10^{-4} \, \eta^3.$$

(3.51)

According to Eq. (3.42), the beam with initial Gaussian distribution becomes more uniform when the parameter η is close to 4.

Uniform Irradiation of Large Targets
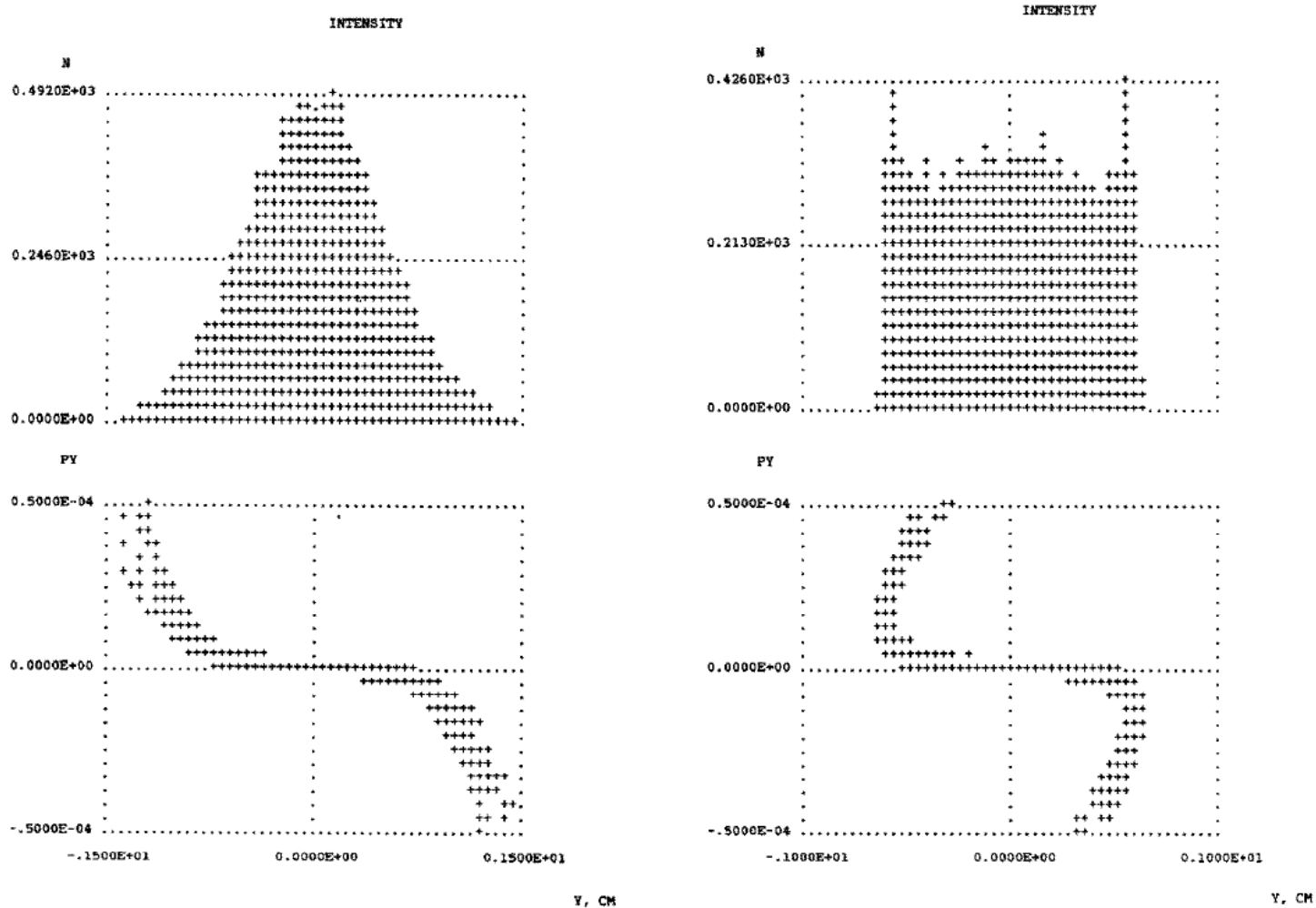
Beam intensity redistribution in the channel with higher order multipoles. Upper part illustrates particle distributions at the beginning (left) and at the end (right) of the transport channel, lower part shows the phase-space projections of the beam.

32

Consider the one-dimensional problem for a beam of particles with charge q and mass m propagating along the z-axis with a longitudinal velocity $v_z = \beta_z c$. Suppose that a particle at $z = 0$ has the velocity modulation:

$$v_x = v_{x0} + a_2 x_0 + a_3 x_0^2 + a_4 x_0^3 + \cdots + a_n x_0^{n-1}, \quad (1)$$

where v_{x0} and x_0 are the initial transverse velocity and position of the particle, a_2 is a linear modulation coefficient, and a_3, $a_4, \ldots$ are nonlinear modulation coefficients. After a drift of the beam the x-coordinate of the particle at any z is

$$x = x_0 + \frac{z}{v_z} \left(v_{x0} + a_2 x_0 + a_3 x_0^2 + a_4 x_0^3 + \cdots \right). \quad (2)$$

The number of particles dN inside the element $(x, x + dx)$ is invariable, hence the particle density $\rho(x) = dN/dx$ at any z is connected with the initial density $\rho(x_0)$ by

$$\rho(x) = \rho(x_0) \frac{dx_0}{dx} \quad (3)$$

or

$$\rho(x) = \rho(x_0)\left(1 + \alpha_2 + 2\alpha_3 x_0 + 3\alpha_4 x_0^2 + 4\alpha_5 x_0^3\right.$$
$$\left. + \cdots (n-1)\alpha_n x_0^{n-2}\right)^{-1}, \quad (4)$$

where $\alpha_n = a_n z/v_z$. From eq. (4) it follows that redistribution of the particle density can be obtained using the nonlinear velocity modulation coefficients α_3, α_4, $\alpha_5 \cdots$ while the linear modulation coefficient α_2 only scales the density.
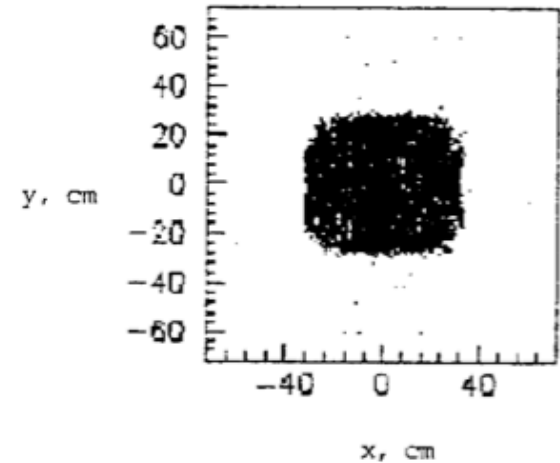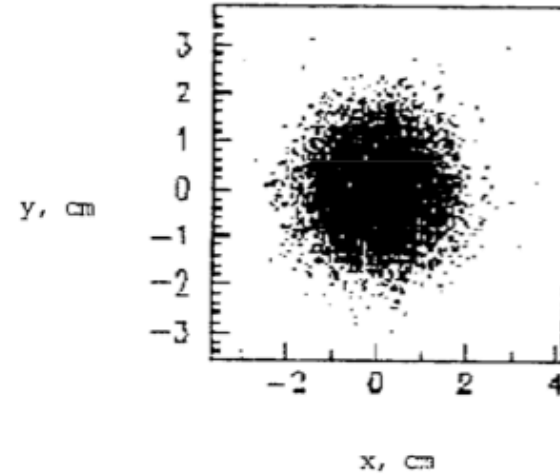
Fig. 1. Projections of computer simulation using code BEAMPATH [7] into real space (x-y) for an initial (upper) and final (lower) beam distribution in a non-linear optics channel.

33

Experimental Observation of Beam Profile Uniforming
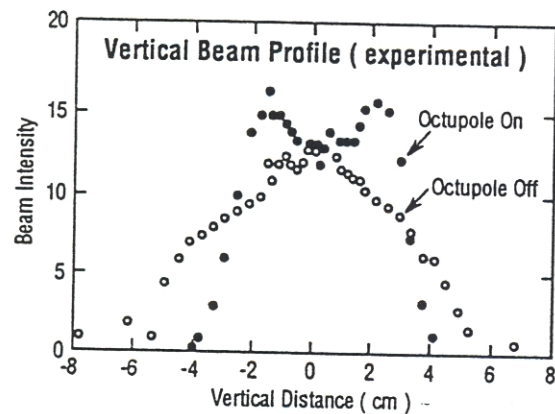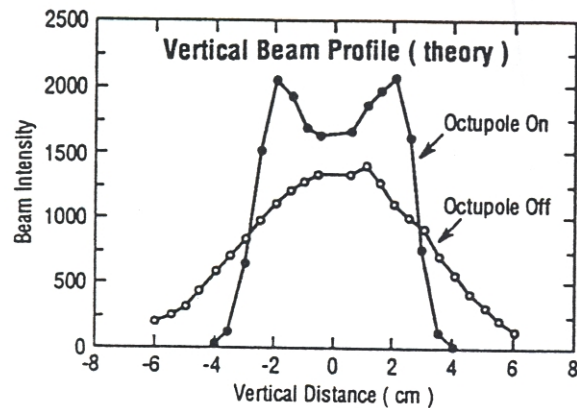
Theoretical calculations (top graph) and the experimental results (bottom graph) of the vertical beam profiles at the target location of the REF facility, with octupoles on and off.
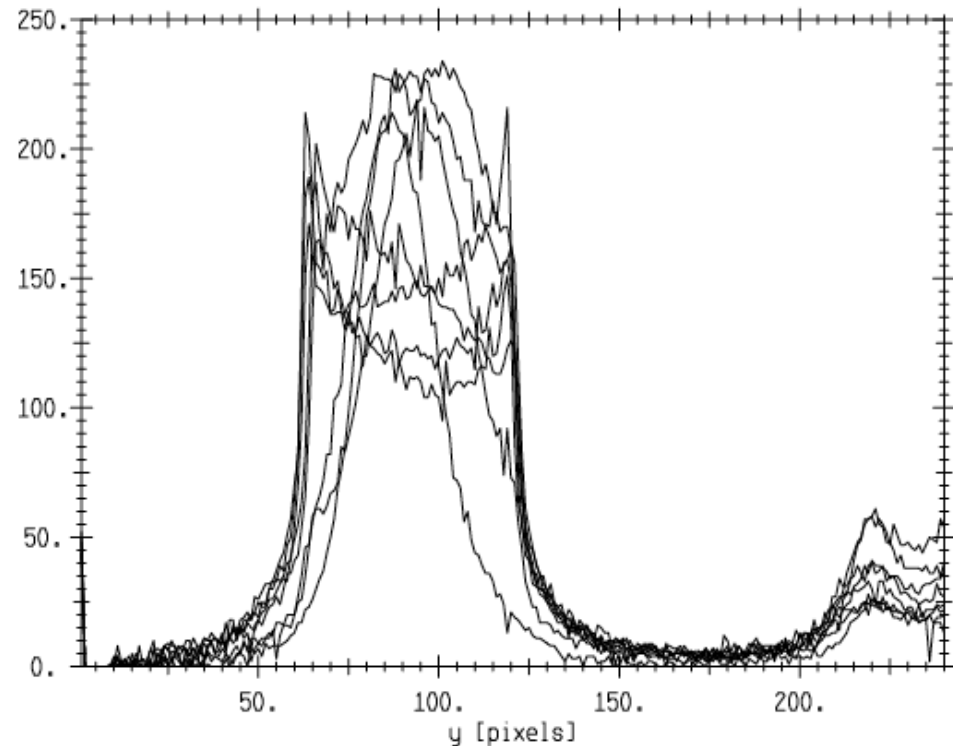
Observed beam profile at LANL beam expander experiment (1997).

REF (Radiation Effects Facility, 200 MeV H- BNL Linac)

Beam Emittance Growth in a Focusing Channel

z = 0

z = 30 cm

z = 104 cm
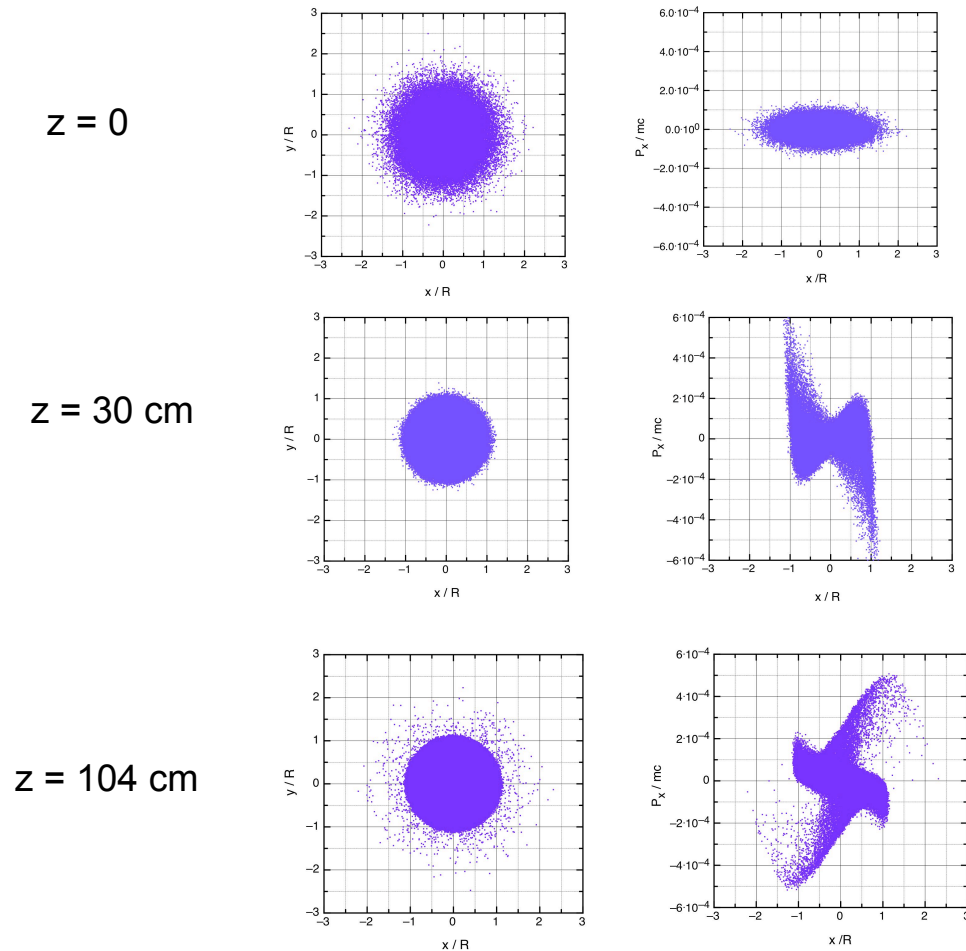
Fig. 3.7. Injection of 135 keV, 100 mA, 0.07 π cm mrad proton beam with Gaussian distribution in a focusing channel with linear field. It results in (a) beam uniforming
(b) beam emittance growth
(c) halo formation.

Conservation of energy for electromagnetic field (Umov-Poynting's theorem)

$$\oint_S [\vec{E},\vec{H}]d\vec{S} = -\frac{d}{dt}\int_V (\frac{\mu_o H^2}{2} + \frac{\varepsilon_o E^2}{2})dV - \int_V \vec{j}\vec{E}\,dV \qquad (3.52)$$
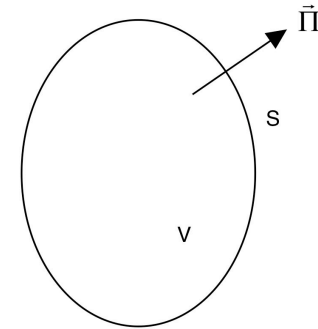
Expression on the left side is an integral of Poynting's vector

$$\vec{\Pi} = [\vec{E},\vec{H}] \qquad (3.53)$$

over surface *S* surrounding volume *V* and is equal to the power of electromagnetic irradiation, or energy of electromagnetic field coming through the surface *S* per second. The first integral in right side of Eq. (3.52) is a change of energy of electromagnetic field per second:

$$\frac{dW}{dt} = \frac{d}{dt}\int_V (\frac{\mu_o H^2}{2} + \frac{\varepsilon_o E^2}{2})dV \qquad (3.54)$$

where electromagnetic energy in volume *V* is

$$W = \frac{1}{2}\int_V (\mu_o H^2 + \varepsilon_o E^2)dV \qquad (3.55)$$

Second term in right side of Eq. (3.52) can be expressed as a sum over all charges in the beam

$$\int_V \vec{j}\vec{E}\,dV = \int_V \rho\vec{v}\vec{E}\,dV = \sum q\vec{v}\vec{E} \tag{3.56}$$

Change of kinetic energy $W_{kin} = mc^2(\gamma - 1)$ of particle in time is

$$\frac{dW_{kin}}{dt} = mc^2\frac{d\gamma}{dt} \tag{3.57}$$

where derivative of reduced particle energy $\gamma = \sqrt{1 + (p/mc)^2}$ over time is

$$\frac{d\gamma}{dt} = \frac{1}{\gamma(mc)^2}\vec{p}\frac{d\vec{p}}{dt} = \frac{1}{mc^2}\vec{v}\frac{d\vec{p}}{dt} = \frac{1}{mc^2}q\vec{v}\vec{E} \tag{3.58}$$

Therefore,

$$q\vec{v}\vec{E} = \frac{dW_{kin}}{dt} \tag{3.59}$$

and second term, Eq. (3.52), is the change of kinetic energy of the beam in time:

$$\sum q\vec{v}\vec{E} = \sum \frac{dW_{kin}}{dt} \tag{3.60}$$

Consider non-relativistic case (no magnetic field):

$$\frac{d}{dt}(\frac{\varepsilon_o}{2}\int E^2 \, dV + \sum_{i=1}^{N} W_{kin}) = 0 \quad , \tag{3.61}$$

where E is the total electrostatic field in the structure, and W_{kin} is the kinetic energy of particle:

$$W_{kin} = mc^2 \sqrt{1 + \frac{p_x^2 + p_y^2 + p_z^2}{(mc)^2}} \approx mc^2\gamma + \frac{p_x^2 + p_y^2}{2m\gamma} \tag{3.62}$$

and summation in Eq. (3.61) is performed over all particles of the beam. Assume that energy is the same for all particles, and is not changed during beam transport. Below consider only transverse particle motion and kinetic energy, associated with this motion. According to definition of rms beam values, kinetic energy of particles is:

$$\sum_{i=1}^{N} W_{kin} = \frac{N}{2m\gamma} [<p_x^2> + <p_y^2>] \, . \tag{3.63}$$

where rms value of transverse momentum is $\qquad <p_x^2> = (\frac{mc\varepsilon}{2R})^2 \, . \tag{3.64}$

In a round beam rms values in both transverse directions are the same, $<p_x^2> = <p_y^2>$, therefore

$$\sum_{i=1}^{N} W_{kin} = N\frac{mc^2}{\gamma}(\frac{\varepsilon}{2R})^2 \, . \tag{3.65}$$

We consider continuous beam, therefore Eq. (3.61) can be rewritten as

$$L_b \frac{\varepsilon_o}{2} \int_o^\infty E^2 \, dS + N \frac{mc^2}{\gamma} (\frac{\varepsilon}{2R})^2 = const \quad ,$$

(3.66)

where L_b is an arbitrary length along the beam, containing N particles. Using beam current $I = q\beta cN/L_b$, Eq. (3.66) becomes:

$$\frac{4q\gamma \beta c}{mc^2 I} (\frac{\varepsilon_o}{2} \int_0^\infty E^2 dS) + (\frac{\varepsilon}{R})^2 = const$$

(3.67)

Applying the last equation to the initial and final beam, one has,

$$\frac{\varepsilon_f^2}{\varepsilon_i^2} = \frac{R_f^2}{R_o^2} + \frac{4q\gamma \beta c R_f^2}{mc^2 I \varepsilon_i^2} (\frac{\varepsilon_o}{2} \int_o^\infty E_i^2 \, dS - \frac{\varepsilon_o}{2} \int_o^\infty E_f^2 \, dS) \quad .$$

(3.68)

Eq. (3.68) can be rewritten as

$$\frac{\varepsilon_f^2}{\varepsilon_i^2} = \frac{R_f^2}{R_o^2}(1 + b\frac{W_i - W_f}{W_o}),$$ (3.69)

where initial, W_i, and final, W_f, energy stored in electrostatic field are

$$W_i = \frac{\varepsilon_o}{2}\int_o^\infty E_i^2\, dS \quad W_f = \frac{\varepsilon_o}{2}\int_o^\infty E_f^2\, dS,$$ (3.70)

and normalization constant is

$$W_o = 2\pi\varepsilon_o(\frac{I}{I_c}\frac{mc^2}{q\beta\gamma})^2$$ (3.71)

If the beam is initially rms-matched, then the rms beam radius is changing insignificantly, so we can put $R_f \approx R_o$. Additionally, taking into account expression

$$b = \frac{\mu_o^2}{\mu^2} - 1$$

one can write:

$$\frac{\varepsilon_f}{\varepsilon_i} = \sqrt{1 + (\frac{\mu_o^2}{\mu^2} - 1)(\frac{W_i - W_f}{W_o})}.$$ (3.72)

In emittance-dominated regime $\mu \approx \mu_o$, and Eq. (3.72) gives us conservation of beam emittance. Consider space charge dominated regime. Initial total field E_i is given by:

$$E_i = \frac{mc^2}{qR\gamma} \frac{2I}{\beta\gamma I_c} \{- \frac{r}{R} + \frac{R}{r} [1 - exp(-\frac{2r^2}{R^2})]\} .$$

(3.73)
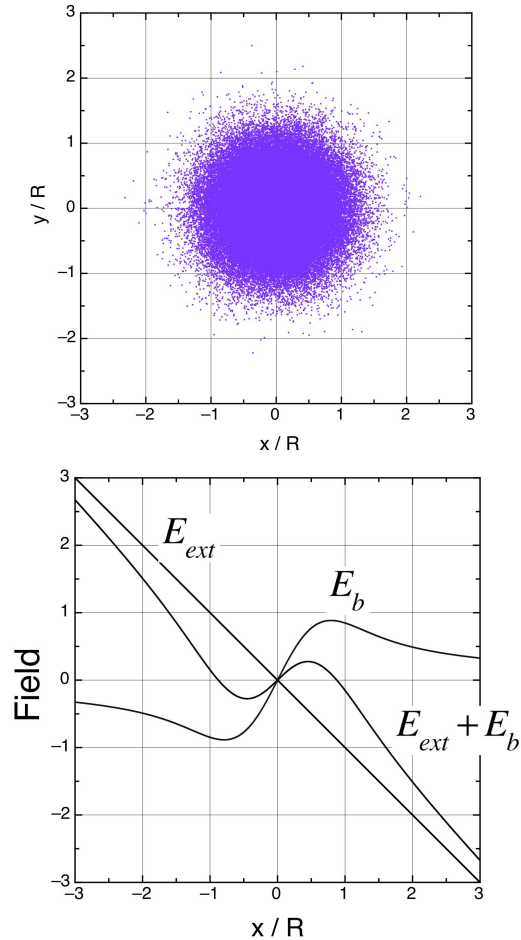
External focusing field E_{ext}, space charge field of Gaussian beam E_b, and total field $E_{ext} + E_b$ at initial moment of time.

Final beam distribution is close to uniform with the same value of beam radius R. It is a general property of space-charge dominated regime, that self-field of the beam almost compensates for external field within the beam. We can put $E_f \approx 0$ within the beam and $E_f = E_{ext} + E_b$ outside the beam

$$E_f = \left\{ \begin{array}{ll} 0, & r \leq R \\ \dfrac{mc^2}{qR} \dfrac{2I}{\beta\gamma^2 I_c} \left(-\dfrac{r}{R} + \dfrac{R}{r}\right), & r > R \end{array} \right. \tag{3.74}$$
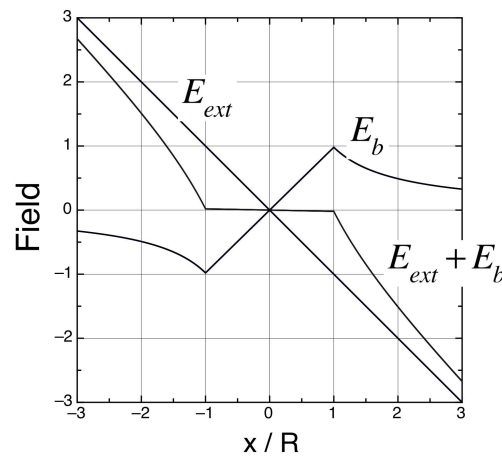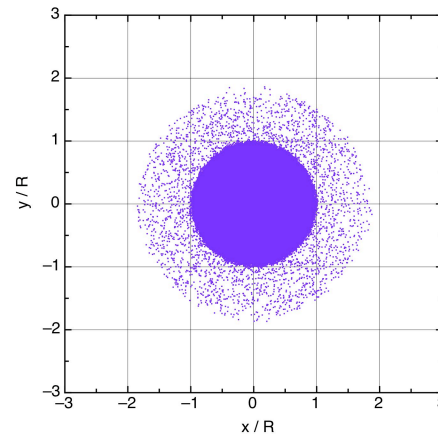
External focusing field E_{ext}, space charge field E_b, and total field $E_{ext} + E_b$ after beam uniforming.

42

Substitution of E_f and E_i into Eq.(3.70) gives for

$$\frac{W_f - W_i}{W_o} = \int_o^{\xi_{max}} [-\xi + \frac{1}{\xi}(1 - e^{-2\xi^2})]^2 \xi d\xi - \int_1^{\xi_{max}} (-\xi + \frac{1}{\xi})^2 \xi d\xi \approx 0.077$$

(3.75)

where $\xi = r / R$. In Eq. (3.75) the upper limit of integration is arbitrary and usually is determined by the aperture of the channel, $\xi_{max} = a / R$.

Free energy parameter for different beam distributions

4D Distribution	2D Projection	$\dfrac{W_i - W_f}{W_o}$
KV	ρ_o	0
Water Bag	$\rho_o(1 - \dfrac{r^2}{R^2})$	0.01126
Parabolic	$\rho_o(1 - \dfrac{r^2}{R^2})^2$	0.02366
Gaussian	$\rho_o \exp(-\dfrac{r^2}{R^2})$	0.077
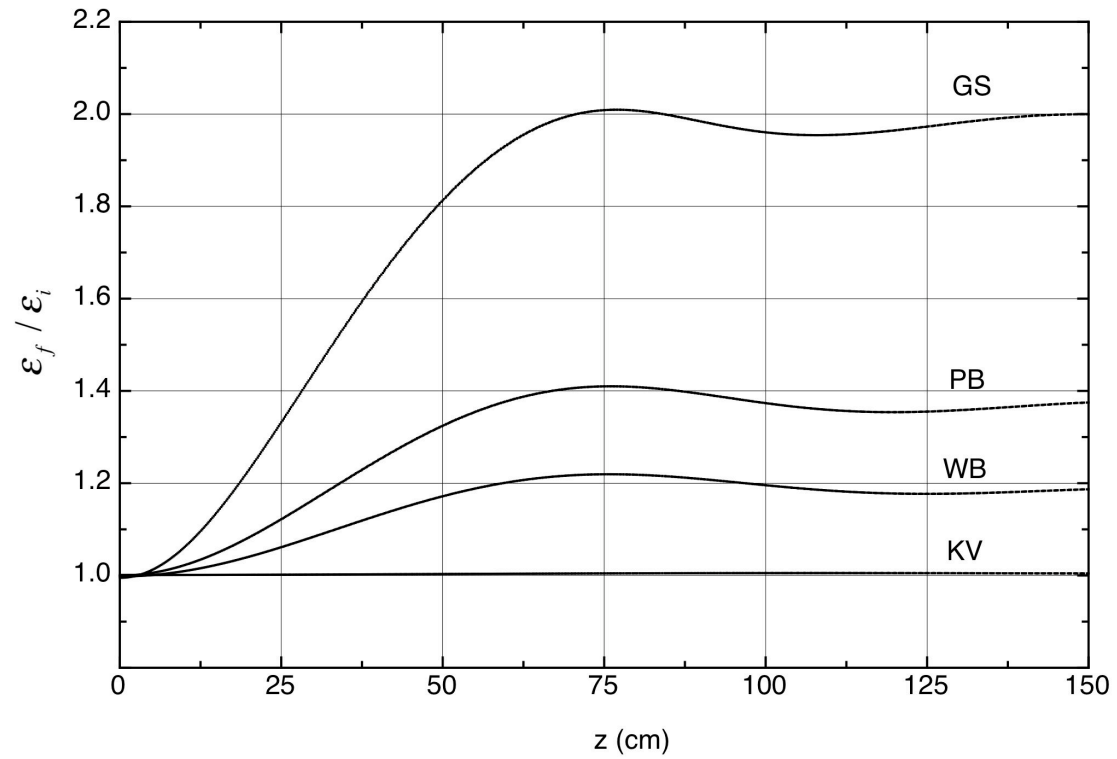
Beam emittance growth in a uniform focusing channel for different particle distributions.

Reduction of Beam Emittance Growth due to Free-Energy Effect

Emittance growth due to free-energy effect

$$\frac{э_{eff}}{э} = \frac{R_f}{R}\sqrt{1+(\frac{\mu_o^2}{\mu^2}-1)\frac{\Delta W}{W_o}}$$

1. Rms beam matching

$$R_f = R$$

2. Reduction of beam size (using higher RF frequency for RF linac)

$$\frac{\mu_o^2}{\mu^2}-1 = \frac{1}{(\beta\gamma)^3}\frac{I}{I_c}(\frac{R}{э})^2$$
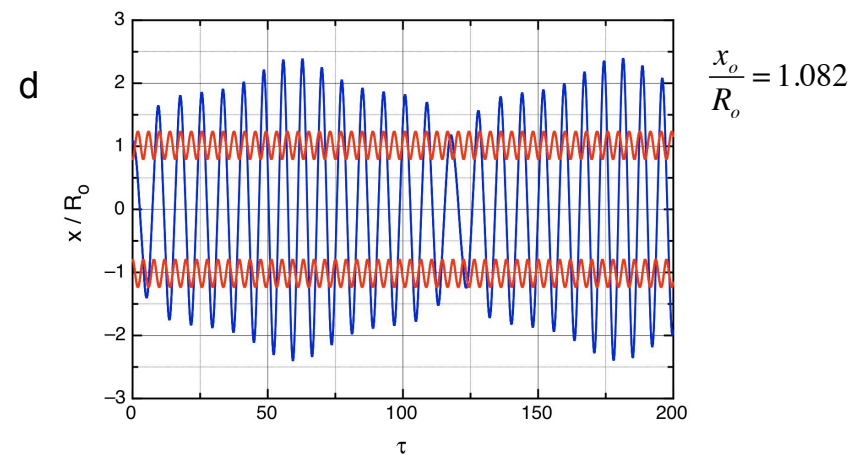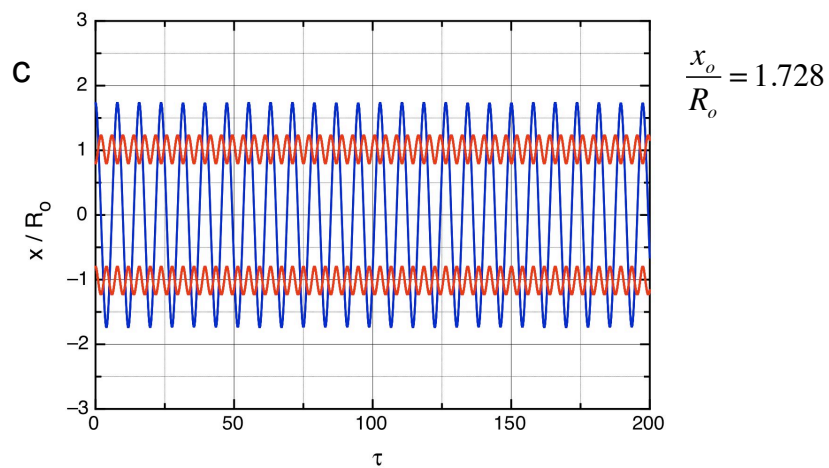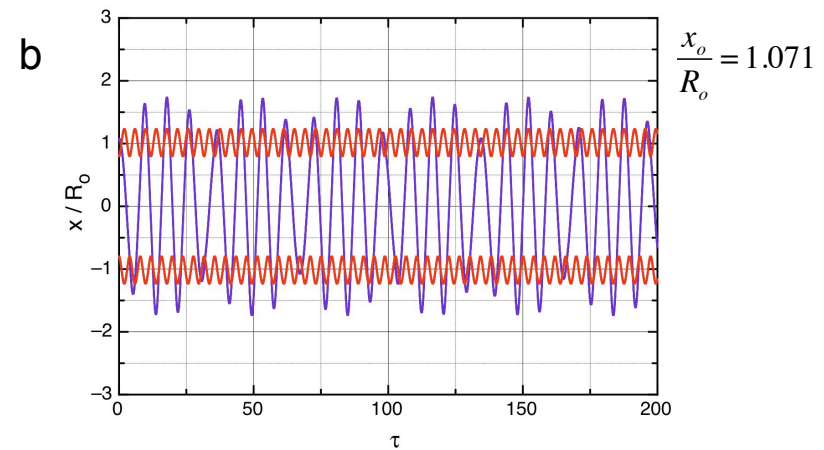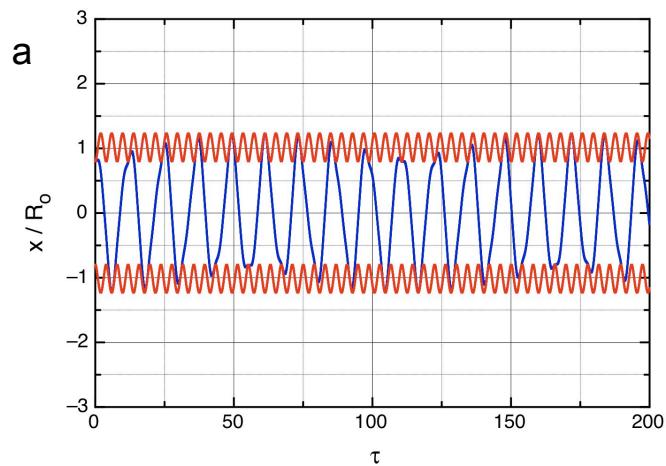
Envelope oscillations of the beam with space charge parameter b=3, amplitude Δ = 0.2 and single particle trajectories with initial conditions (a) x_o/R_o=0.8, (b) x_o/R_o =1.071, (c) x_o/R_o =1.728, (d) x_o/R_o =1.082.

46

Stroboscopic Particle Motion
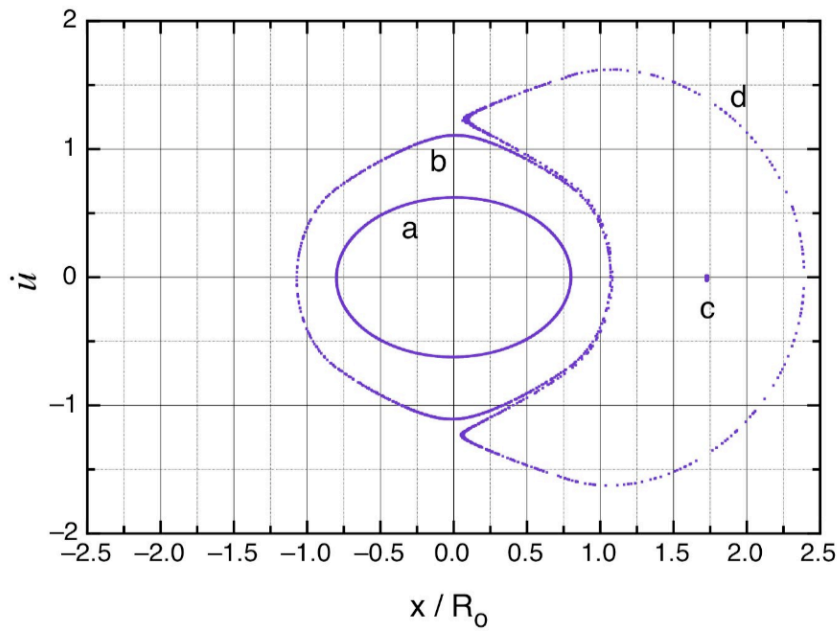
Stroboscopic particle trajectories at phase plane $(u,\, du\,/\,d\tau)$ taken after each two envelope oscillation periods: (a) x_o/R_o=0.8, (b) x_o/R_o=1.071, (c) x_o/R_o=1.728, (d) x_o/R_o=1.082.

Particle – Core Model

Dimensionless $r = \dfrac{R}{R_e}$ beam envelope (core) equation: $\dfrac{d^2 r}{d\tau^2} + r - \dfrac{1}{(1+b)r^3} - \dfrac{b}{(1+b)r} = 0$

Single particle equation of motion $u = \dfrac{x}{R_e}$:
$$\frac{d^2 u}{d\tau^2} + u = \begin{cases} \dfrac{b}{(1+b)}\dfrac{u}{r^2}, & |u| \leq r \\[2mm] \dfrac{b}{(1+b)u}, & |u| > r \end{cases}$$

Space charge parameter

$$\boxed{b = \frac{2}{\beta\gamma}\frac{I}{I_c}\frac{R_e^2}{\varepsilon^2}}$$

I beam current

$I_c = 4\pi\varepsilon_o mc^3 / q$ characteristic beam current

ε normalized beam emittance

β particles velocity,

γ particle energy

R_o radius of the equilibrium envelope

Small intensity beam $b \approx 0$

High intensity beam b >> 1

Approximation of Space Charge Field
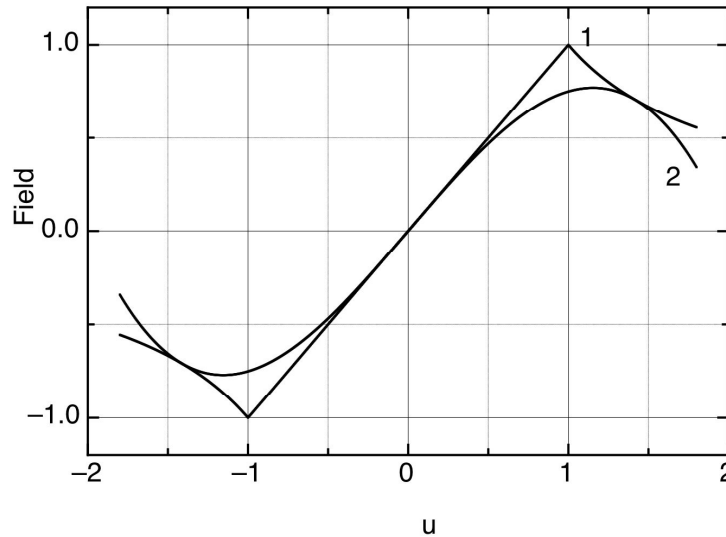
(1) Field of uniformly charged beam

(2) Field approximation:

$$F = \frac{b}{(1+b)} \begin{cases} \dfrac{u}{r^2}, & |u| \le r \\[2mm] \dfrac{1}{u}, & |u| > r \end{cases}$$

$$F = \frac{b}{(1+b)}\left(-\frac{u}{r^2} + \frac{u^3}{4}\right)$$

Envelope Oscillations

Envelope equation

$$\frac{d^2 r}{d\tau^2} + r - \frac{1}{(1+b)r^3} - \frac{b}{(1+b)r} = 0$$

Expansions
$$r = 1 + \vartheta \qquad \frac{1}{r} \approx 1 - \vartheta \qquad \frac{1}{r^3} \approx 1 - 3\vartheta \qquad \frac{d^2 \vartheta}{d\tau^2} + 2(\frac{2+b}{1+b})\vartheta = 0$$

Equation for small deviation from equilibrium

$$r = 1 + \Delta\cos(2\Omega\tau)$$

Envelope oscillation frequency

$$2\Omega = \sqrt{2(\frac{2+b}{1+b})}$$

For small intensity beam $b \approx 0$ $\qquad r = 1 + \Delta\cos 2\tau$

For high intensity beam b >>1 $\qquad r = 1 + \Delta\cos\sqrt{2}\tau$
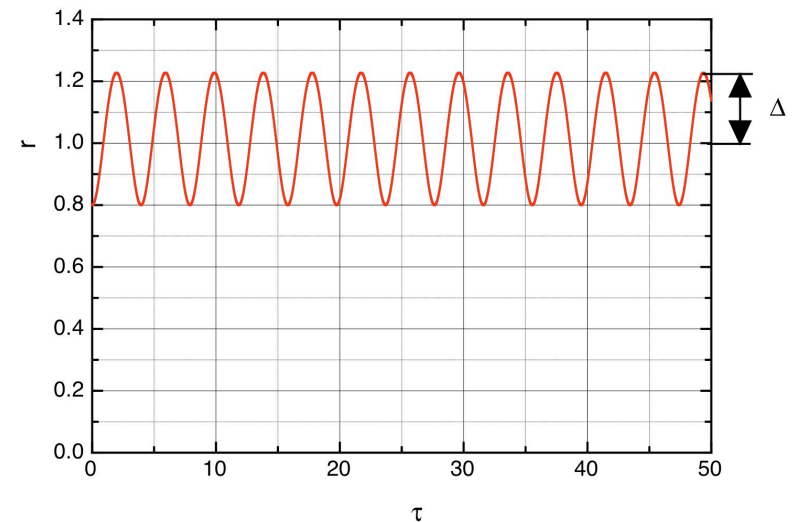
Anharmonic Oscillator with Parametric Excitation for Single Particle Motion

With field approximation, equation of particle motion is

$$\frac{d^2u}{d\tau^2} + u - \left(\frac{b}{1+b}\right)\left[\frac{u}{(1+\Delta\cos 2\Omega\tau)^2} - \frac{u^3}{4}\right] = 0$$

Using expansion

$$\frac{1}{(1+\Delta\cos 2\Omega\tau)^2} \approx 1 - 2\Delta\cos 2\Omega\tau$$

Equation of particle motion

$$\frac{d^2u}{d\tau^2} + u\left(\frac{1}{1+b}\right)(1+2b\Delta\cos 2\Omega\tau) + \left(\frac{b}{1+b}\right)\frac{u^3}{4} = 0$$

Equation corresponds to Hamiltonian

$$H = \frac{\dot{u}^2}{2} + \varpi^2\frac{u^2}{2}(1 - h\cos 2\Omega\tau) + \alpha\frac{u^4}{4}$$

with the following notations

$$\varpi^2 = \frac{1}{1+b} \qquad h = -2b\Delta \qquad \alpha = \frac{b}{4(1+b)}$$

Canonical Transformation of Hamiltonian

Change the variables ($\dot{u}$, u) to new variables (Q, P) using a
generating function

$$F_2(u,P,\tau) = \frac{uP}{\cos\Omega\tau} - (\frac{P^2}{2\varpi} + \varpi\frac{u^2}{2})tg\Omega\tau$$

Relationships between variables are given by:

$$\begin{cases} Q = \dfrac{\partial F_2}{\partial P} = \dfrac{u}{\cos\Omega\tau} + \dfrac{P}{\varpi}\,tg\Omega\,\tau \\[2em] \dot{u} = \dfrac{\partial F_2}{\partial u} = \dfrac{P}{\cos\Omega\tau} - \varpi\,u\,tg\Omega\,\tau \end{cases}$$

$$\text{or}\quad \begin{cases} u = Q\cos\Omega\,\tau + \dfrac{P}{\varpi}\,\sin\Omega\,\tau \\[2em] \dot{u} = -\varpi\,Q\,\sin\Omega\,\tau + P\cos\Omega\,\tau \end{cases}$$
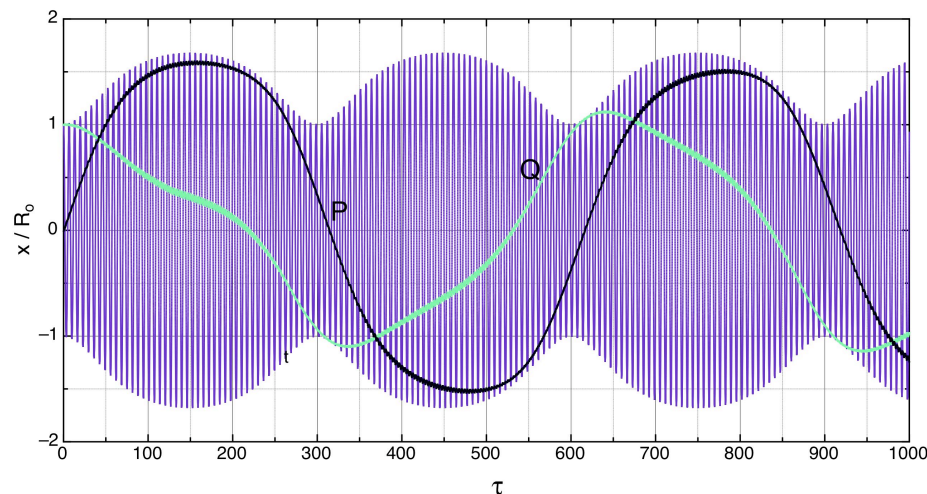
New Hamiltonian $\quad K = H + \dfrac{\partial F_2}{\partial \tau}$

$$K = \frac{P^2}{2} + \varpi^2 \frac{Q^2}{2} - \frac{\varpi^2 h}{2}(Q\cos\Omega\tau + \frac{P}{\varpi}\sin\Omega\tau)^2 \cos 2\Omega\tau + \frac{\alpha}{4}(Q\cos\Omega\tau + \frac{P}{\varpi}\sin\Omega\tau)^4 - \frac{P^2\Omega}{2\varpi} - \frac{\Omega\varpi}{2}Q^2$$

After averaging all time-dependent terms over period of $2\pi/\Omega$

$$\bar{K} = \frac{\varpi^2 \bar{Q}^2}{2}(1 - \frac{\Omega}{\varpi} - \frac{h}{4}) + \frac{\bar{P}^2}{2}(1 - \frac{\Omega}{\varpi} + \frac{h}{4}) + \frac{3}{32}\alpha(\bar{Q}^2 + \frac{\bar{P}^2}{\varpi^2})^2$$

Second Canonical Transformation

Change variables $(\bar{Q}, \bar{P})$ to action-angle variables $(J,\ \psi)$ using generating function

$$F_1(\bar{Q}, \psi) = \frac{\varpi\ \bar{Q}^2}{2\,tg\psi}$$

Transformation is given by

$$\left\{ \begin{array}{l} \bar{Q} = \sqrt{\dfrac{2J}{\varpi}}\ \sin\psi \\[2mm] \bar{P} = \sqrt{2J\varpi}\ \cos\psi \end{array} \right.$$

New Hamiltonian

$$\boxed{\bar{K} = \upsilon J + \kappa J^2 + 2\chi J \cos 2\psi}$$

with the following notations

$$\upsilon = \varpi - \Omega = \frac{\sqrt{2} - \sqrt{2+b}}{\sqrt{2(1+b)}} \qquad \kappa = \frac{3}{32}b \qquad \chi = -\frac{1}{4}\frac{b\Delta}{\sqrt{1+b}}$$

Nonlinear Parametric Resonance

Hamiltonian of averaged motion:
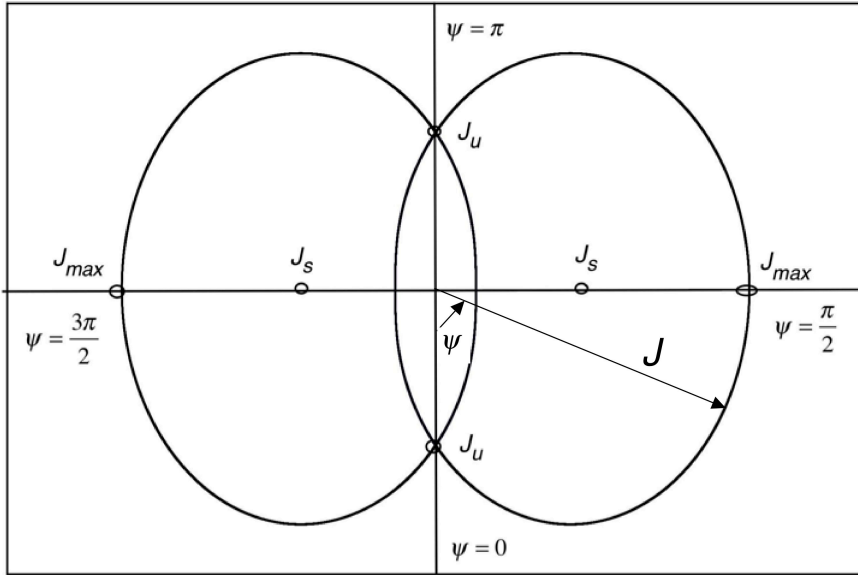
$$\bar{K} = \upsilon J + \kappa J^2 + 2\chi J \cos 2\psi$$

Maximum deviation of particle from the axis

$$\frac{x_{max}}{R_e} = \sqrt{\frac{2J_{max}}{\varpi}}$$

$$J_{max} = \frac{(-\upsilon + 2\chi) + \sqrt{8|\upsilon\chi|}}{2\kappa}$$
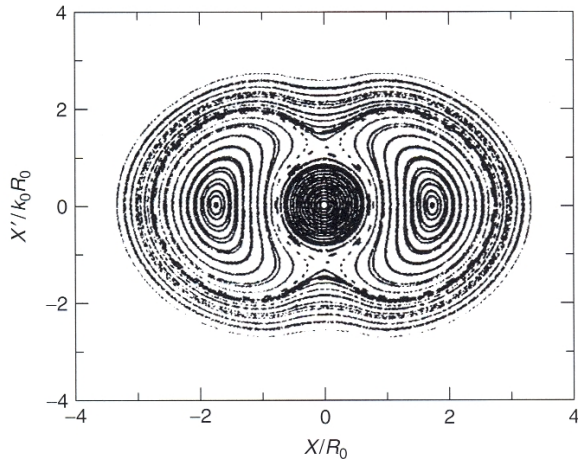
$$\frac{x_{max}}{R_e} = \sqrt{\frac{32}{3} \frac{\sqrt{1 + \frac{b}{2}} - 1 + \frac{b|\Delta|}{2} + \sqrt{2b|\Delta|(\sqrt{1 + \frac{b}{2}} - 1)}}{b}}$$

Figure 9.12 Stroboscopic plot obtained by taking snapshots of many independent particle trajectories, once per core-oscillation cycle at the phase of the core oscillation that gives the minimum core radius. Initial particle coordinates were defined on the x and x′ axes.

55

Comparison of Analytical and Numerical Results
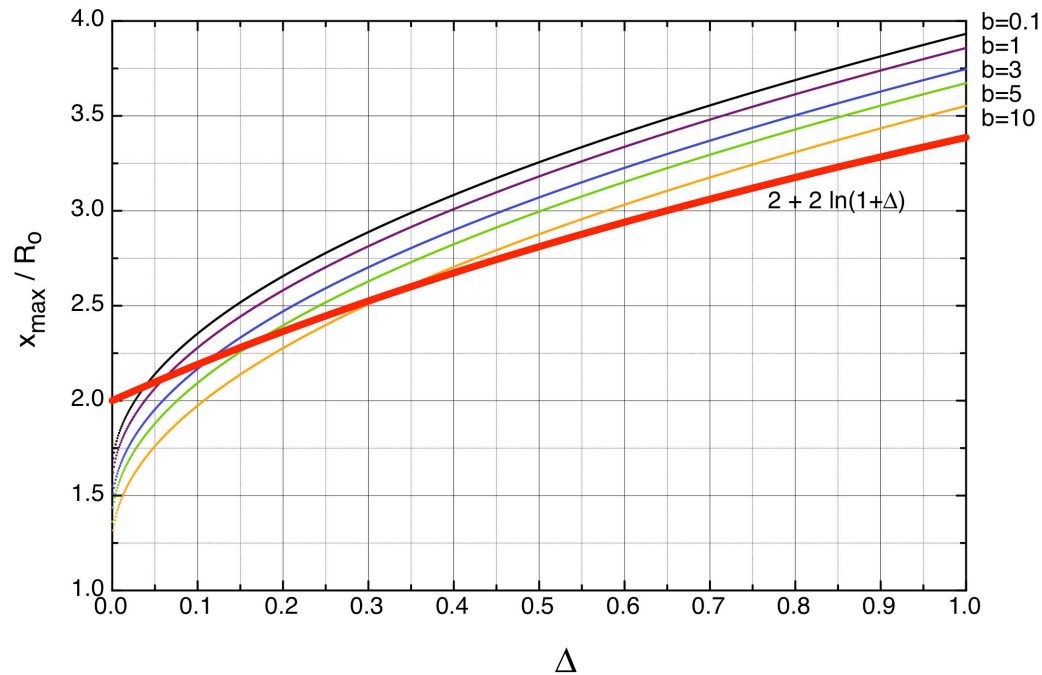
Maximum values of particle deviation from the axis as a function of amplitude of core oscillations (Y.B. NIM-A 618, 2010, p.37). (Red) model of Tom Wangler (*RF Linear Accelerators*, Wiley, 1998)

$$\frac{x_{max}}{R_o/2} = A + B \ln(\mu)$$

where $A = B = 4$, $\mu = 1 + \Delta$.

LANL Beam Halo Experiment (2002)

52 quadrupole FODO lattice

Beam-profile diagnostics in red

RFQ-6.7 MeV

Matching/mismatching
quads Q1 to Q4

Emittances obtained
from measured profiles
at Q20 and Q45
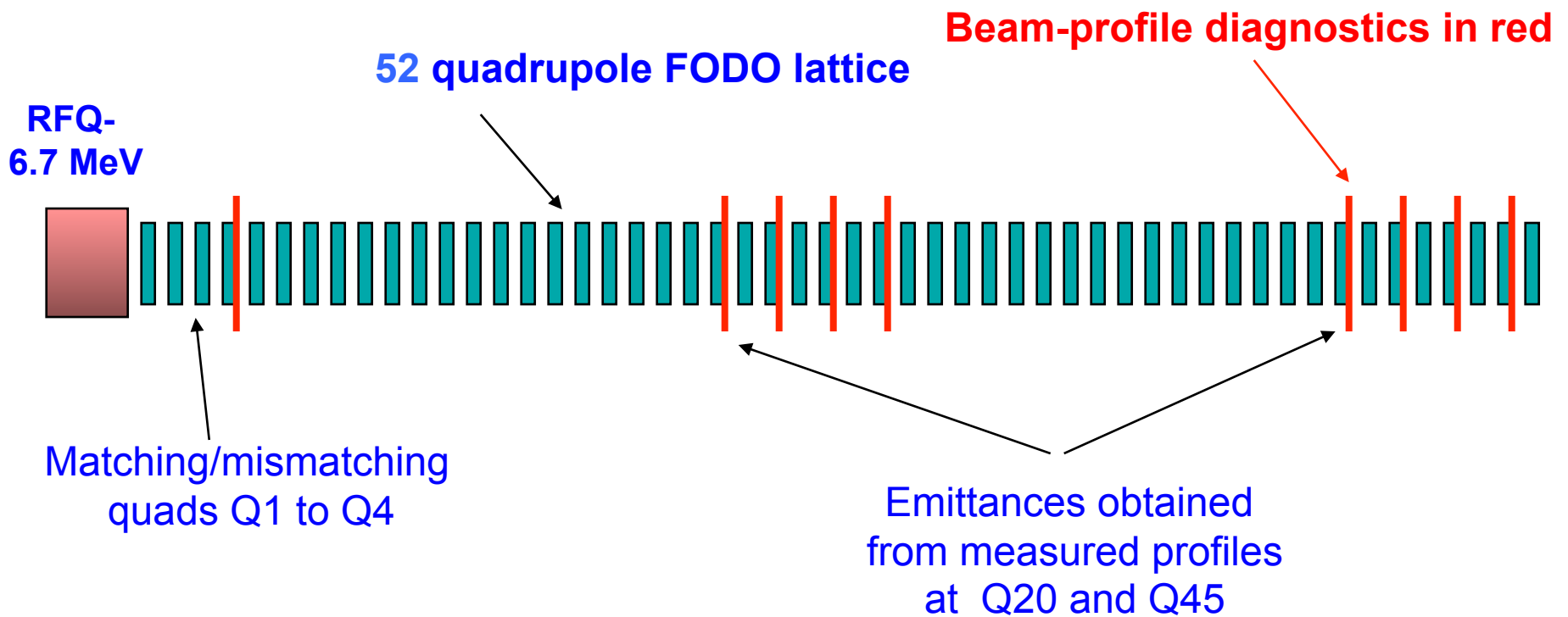
LANL Beam Halo Experiment Lattice
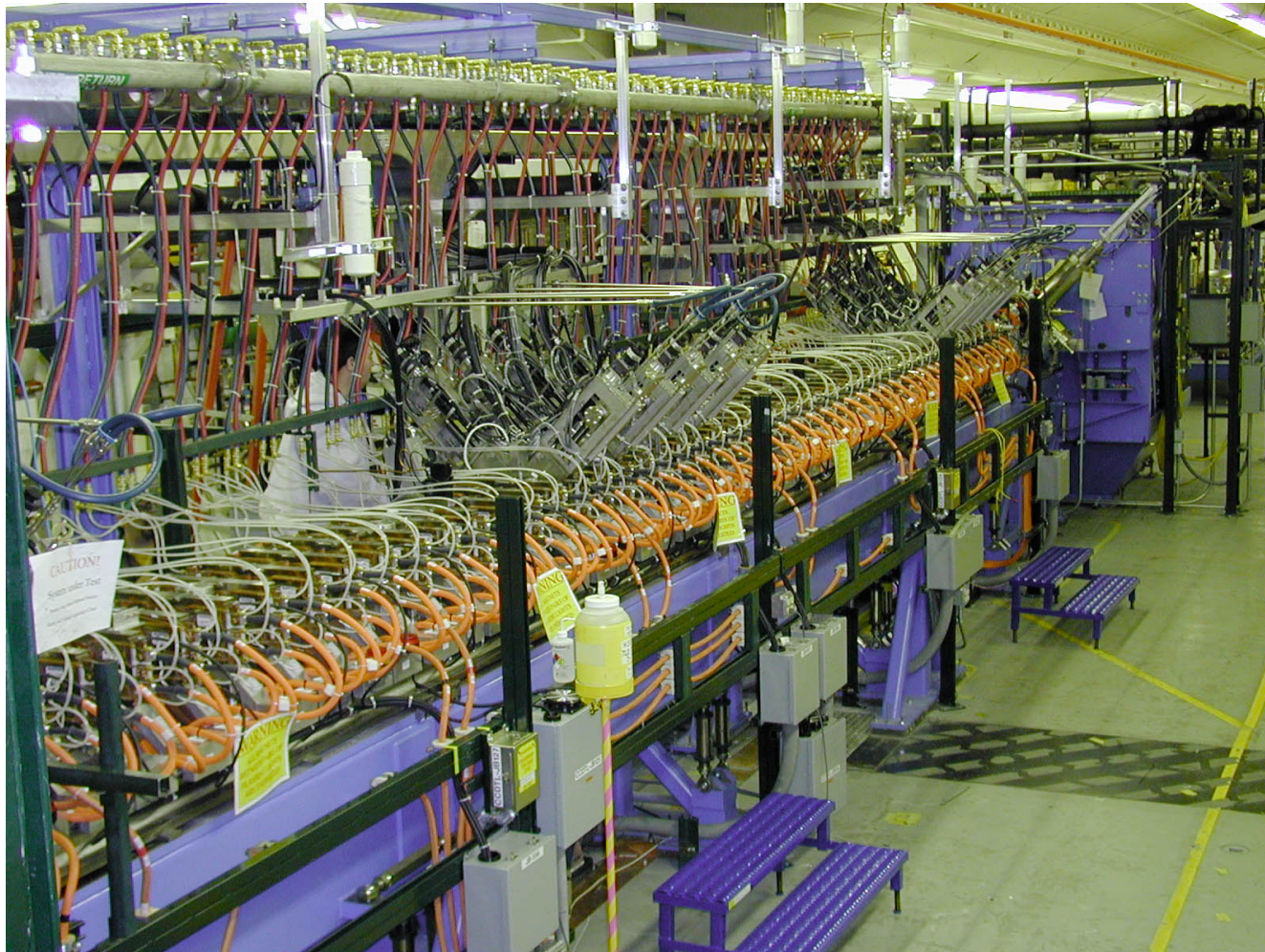
A unique wire and scraper beam-profile diagnostic allowed to measure beam profiles. Gilpatrick, et al.).

- 33–micron carbon wire (too thin to be visible in picture) measures density in beam core above 10^{-3} level.

- Proton range=300 microns so protons pass through wire and make secondary electrons to measure high density in beam core.

- Pair of 1.5mm graphite scraper plates in which protons stop. Can measure proton density outside beam core from 10^{-3} to 10^{-5}.

- Data from wire and scraper plates were combined to produce a single distribution.
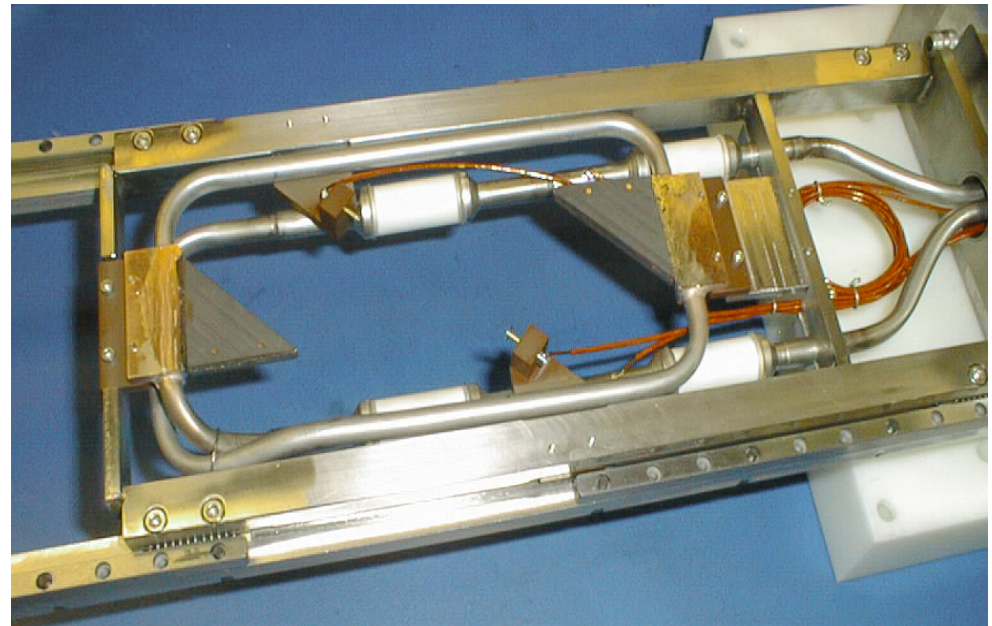
Typical matched beam profile for 75 mA. (m=1,matched)
Shows Gaussian–like core plus low-density halo input beam, observed out to 9 rms.

Linear Plot
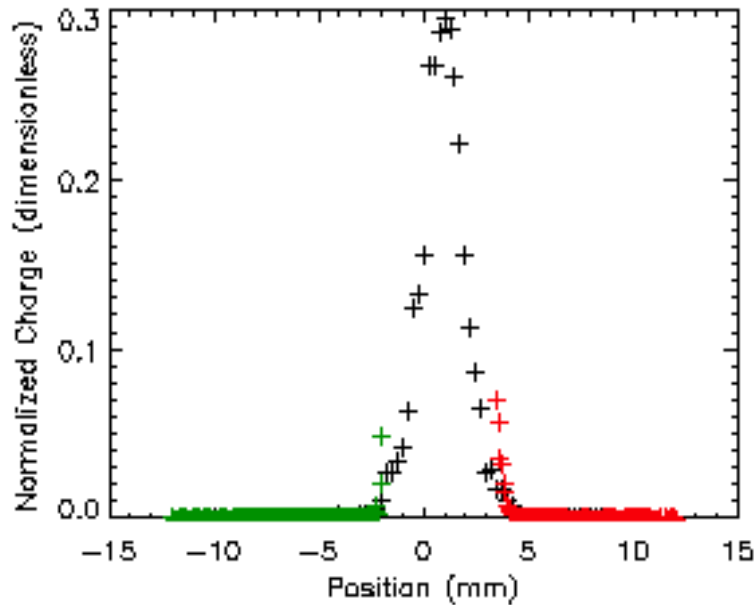
Semilog Plot
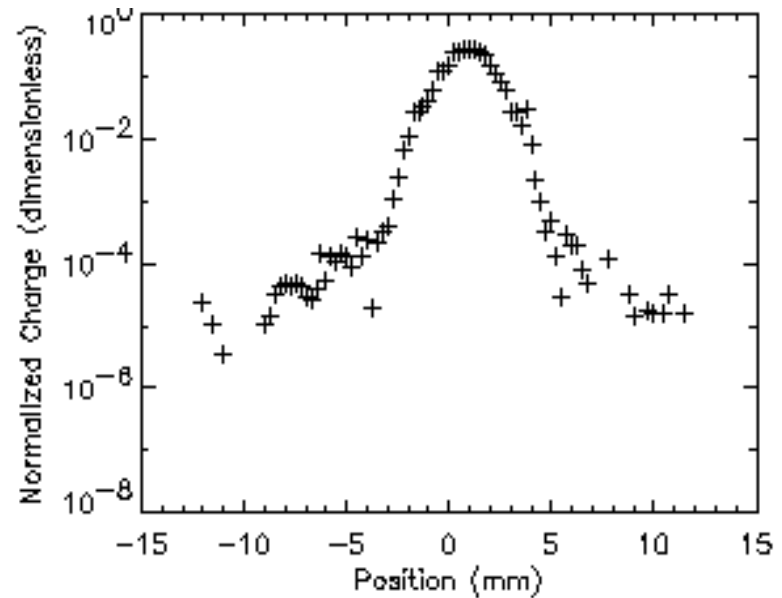
Rapid emittance growth

RMS EMITTANCE GROWTH AT SCANNER #20 - 75 mA - BREATHING MODE
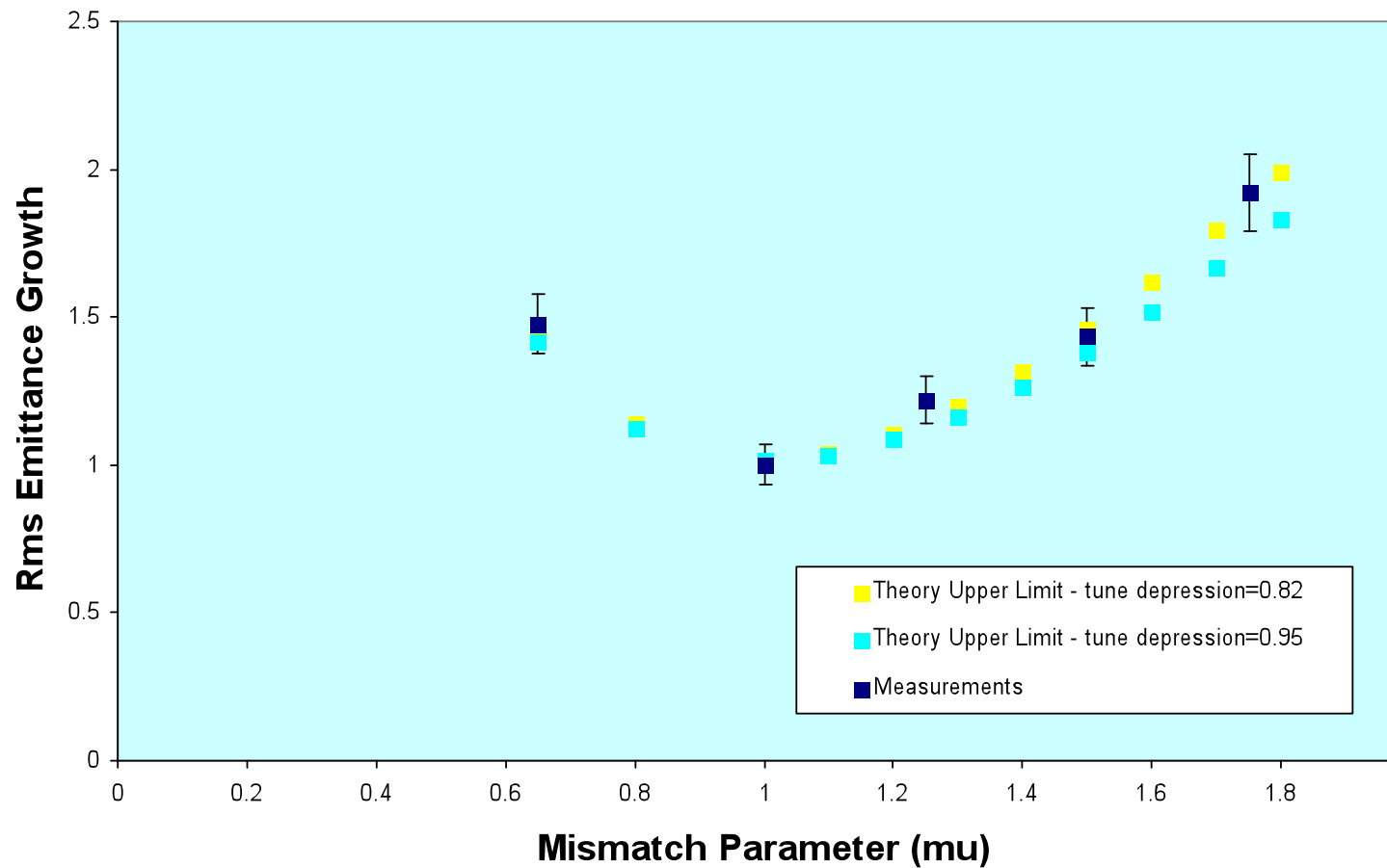
Test of Particle-Core Model
Measurements at different fractional intensity levels (10%, 1%, 0.1%)

Comparison of Measured Beam Widths With Maximum Amplitude
From Particle-Core Model
Scanner 20 - 75 mA - Breathing Mode

62
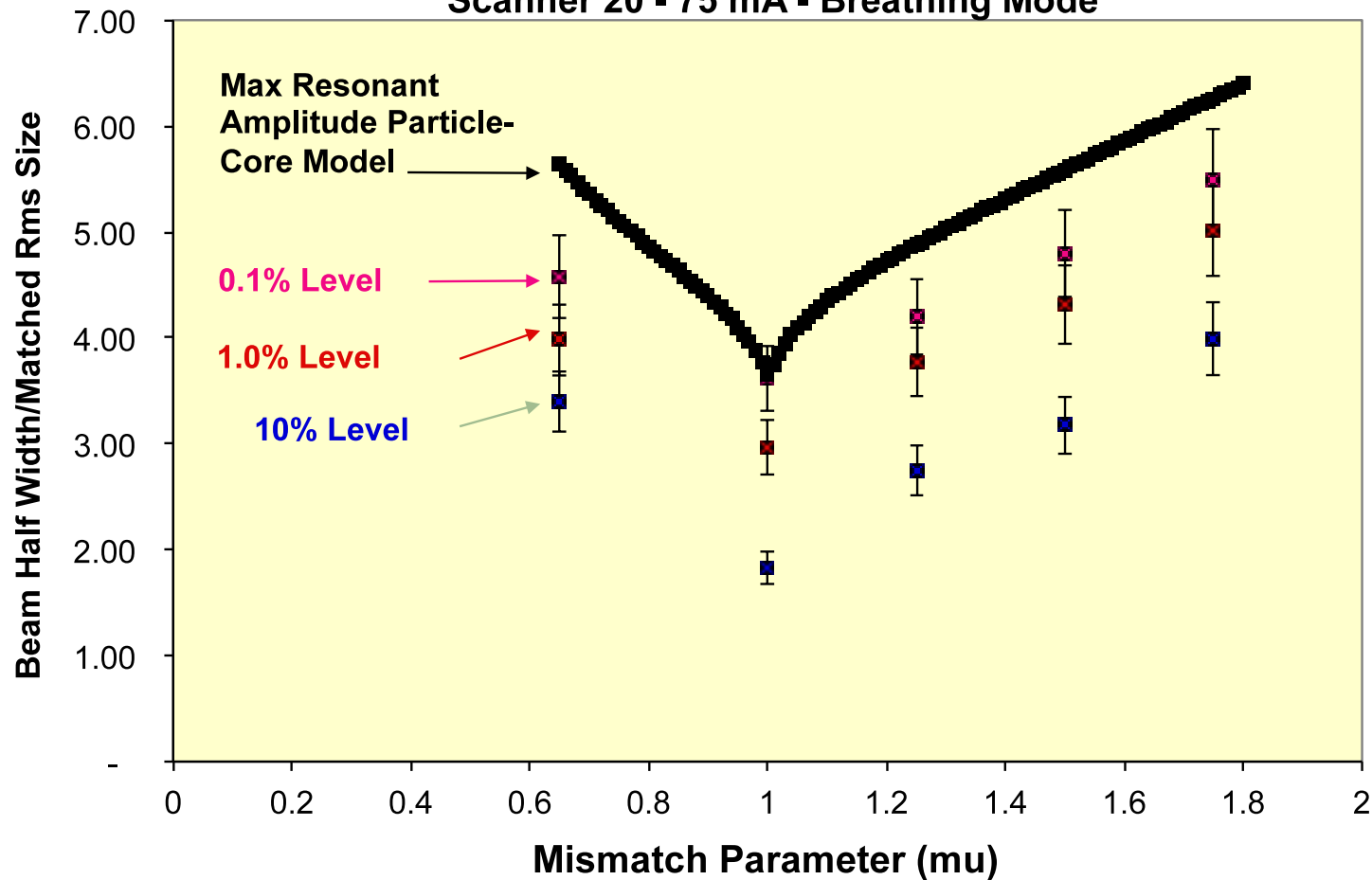
Experimental Observation of Space-Charge Driven Resonances in Linac (L.Groening et al, LINAC2010)

Matched beam envelope

$$R(s, \sigma_{env}) = R_o(\sigma_{env}) + \Delta R(\sigma_{env}) \cdot \cos(\sigma_{env} s)$$

Radial electric field

$$E_r = \frac{18 \cdot I}{\pi \epsilon_o \cdot R(s)^2 \beta c} \left[r - \frac{r^3}{2R(s)^2} + O(r) \right]$$

Single-particle trajectory

or

$$r'' = -\sigma_{\perp,o}^2 r + \frac{e \cdot q}{A \cdot m_u} \cdot E_r$$

Disturbed oscillator with $\sigma_\perp$ as depressed phase advance

$$r'' + \sigma_\perp^2 r \sim |r^3 \cdot e^{i\sigma_{env} s}$$

Resonance condition:

$$\sigma_{env} = 4\sigma_\perp.$$

Phase advance of the matched envelope is 360°, the resonance occurs at $\sigma_\perp$ = 90°

Figure 1: Distribution of particles at the exit of the periodic channel according to the radial particle-core model of the space charge driven transverse 4th-order resonance.

Figure 3: Schematic set-up of the experiments (not to scale).
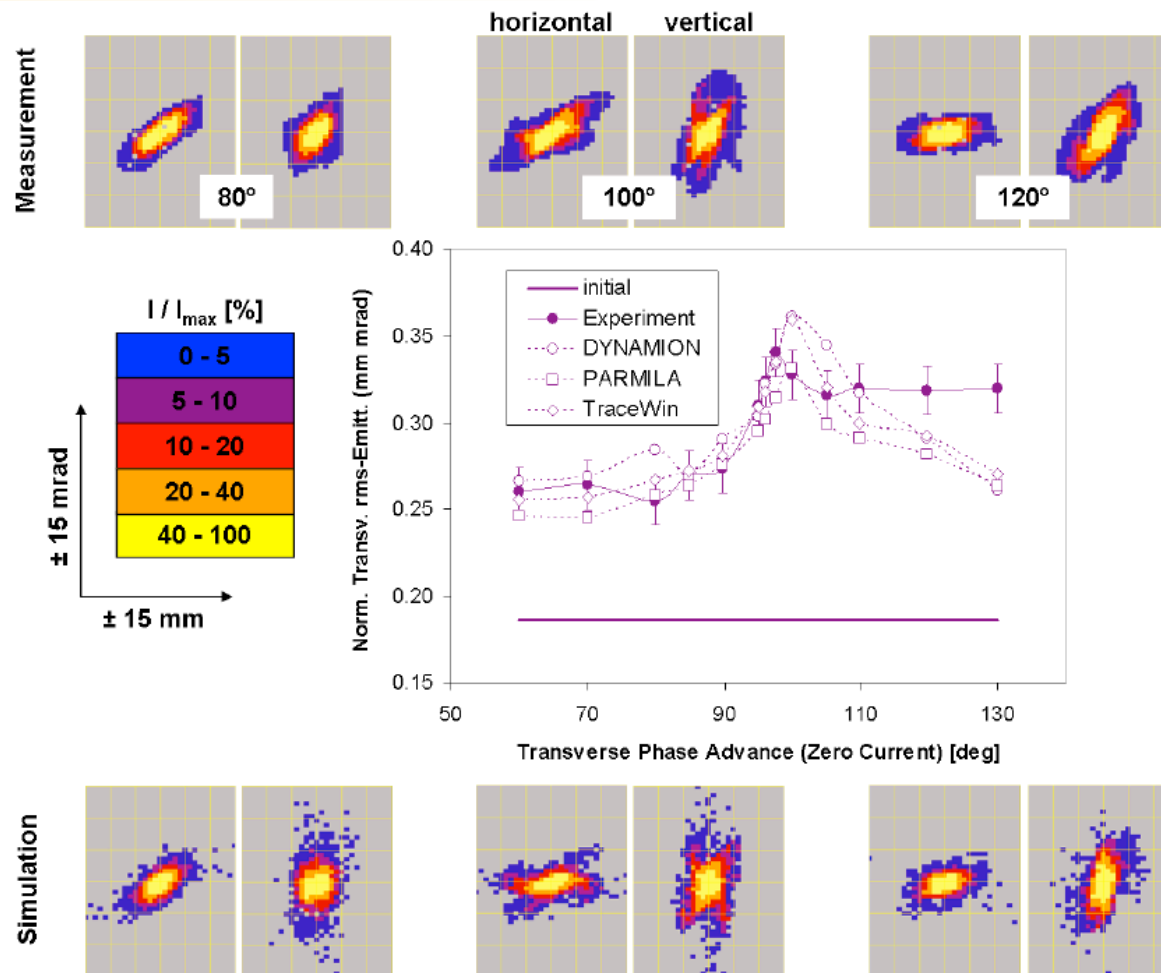
Figure 7: Upper and lower: phase space distributions at the exit of the first DTL tank as obtained from measurements and from the DYNAMION code for phase advances $\sigma_{\perp,o}$ of 80°, 100°, and 120°. Left (right) side distributions refer the horizontal (vertical) plane. The scale is ±15 mm and ±15 mrad. Fractional intensities refer to the phase space element including the highest intensity. Center: Mean of horizontal and vertical normalized rms emittance behind the first DTL tank as a function of the transverse zero current phase advance.

64

Non-uniform beam matching in transport channel

Beam is matched with continuous (z-independent) focusing channel, if beam distribution function $f(x, p_x, y, p_y)$ is constant.

Self-consistent problem:

Vlasov's Equation

$$\frac{df}{dt} = \frac{\partial f}{\partial t} + \frac{\partial f}{\partial \vec{x}} \frac{d\vec{x}}{dt} + \frac{\partial f}{\partial \vec{P}} \frac{d\vec{P}}{dt} = 0$$

Poisson's Equation

$$\Delta U = -\frac{\rho}{\varepsilon_o}$$

Solution:

1. Express distribution function as a function of constant of motion (Hamiltonian) $f = f(H)$. Distribution function automatically obeys Vlasov's equation:

$$\frac{df}{dt} = \frac{\partial f}{\partial H} \frac{\partial H}{\partial t} = 0$$

2. Substitute distribution function into Poisson's equation and solve it.

Non-uniform beam matching in transport channel (cont.)

Two formulations of the self-consistent beam matching problem:

1. The beam distribution function is known (for example, of the beam extracted from the source). The problem is to find focusing potential, which maintains this distribution in the channel:

$$f(x, p_x, y, p_y) \rightarrow U_{ext}(x, y)$$

2. Potential of the focusing structure is given. The problem is to find the beam distribution function, which is maintained in focusing structure:

$$U_{ext}(x, y) \rightarrow f(x, p_x, y, p_y)$$

More info:
Y.B. Phys. Rev. E Vol. 53, No. 5, 5358, 1996;
Y.B. Phys. Rev. E Vol. 57, No. 5, 6020, 1998

Equilibrium of a Gaussian beam

Beam with Gaussian distribution function

$$f = f_o \, exp \left(-2 \, \frac{x^2 + y^2}{R^2} - 2 \, \frac{p_x^2 + p_y^2}{p_o^2} \right)$$
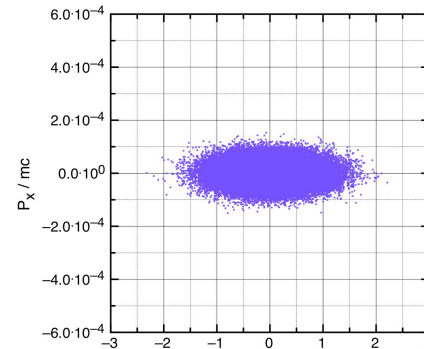
Time-independent Vlasov's equation

$$\frac{mc^2}{q} \frac{1}{\gamma} (x \, p_x + y \, p_y) = \frac{R^4}{\varepsilon^2} \left(p_x \frac{\partial U}{\partial x} + p_y \frac{\partial U}{\partial y} \right)$$

Total potential
$$U(x,y) = \frac{mc^2}{q} \frac{1}{\gamma} \frac{\varepsilon^2}{R^4} \left(\frac{x^2 + y^2}{2} \right)$$

Total field
$$E_{tot} = - \frac{mc^2}{q} \frac{1}{\gamma} \frac{\varepsilon^2}{R^4} \, r$$

Space-charge field
$$E_b = - \frac{\partial U_b}{\partial r} = \frac{I}{2\pi \, \varepsilon_o \, \beta c} \frac{1}{r} [\, 1 - exp(-2 \frac{r^2}{R^2})]$$
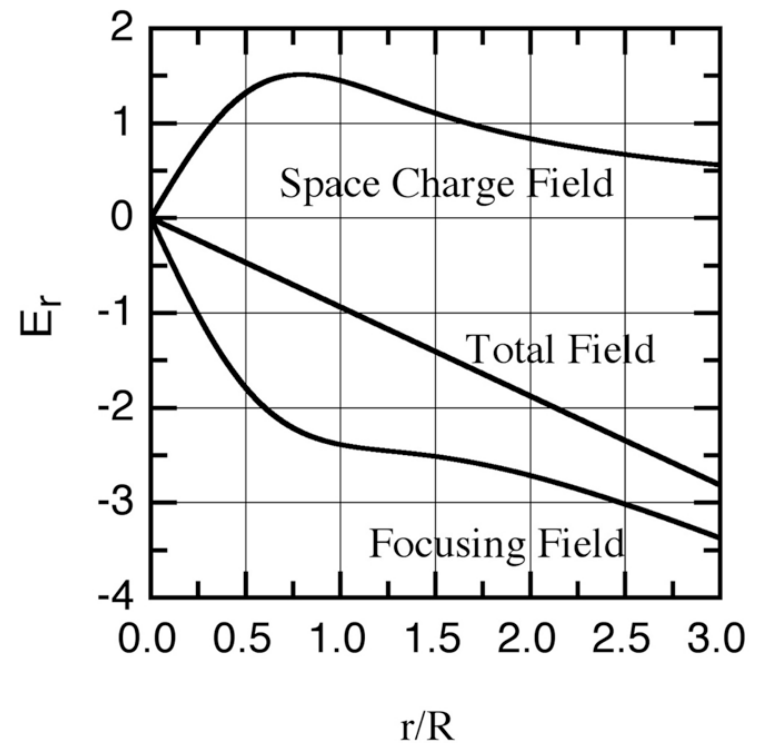
Required focusing field
$$E_{ext} = - \frac{mc^2}{q \, R \, \gamma} \left[\frac{\varepsilon^2 \, r}{R^3} + 2 \frac{I}{I_c \, \beta\gamma} \frac{R}{r} \left(1 - exp \left(-2 \frac{r^2}{R^2} \right) \right) \right]$$
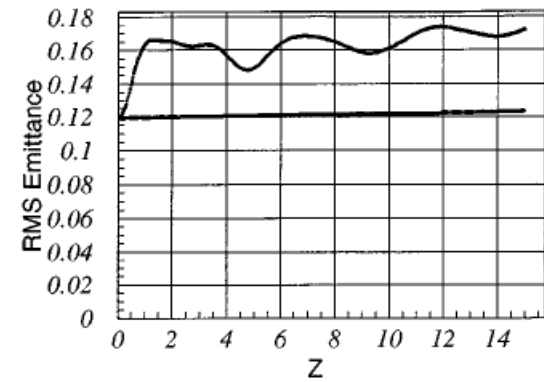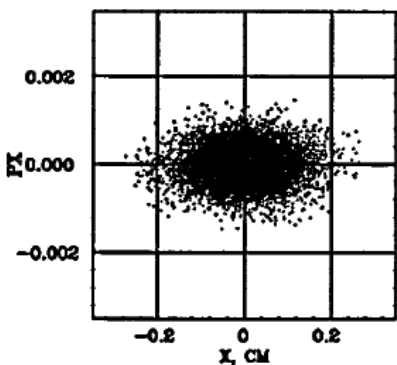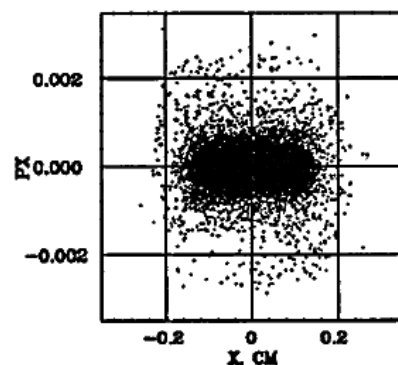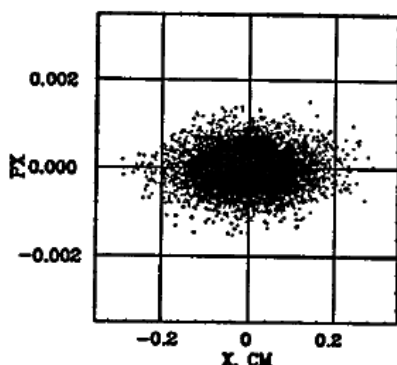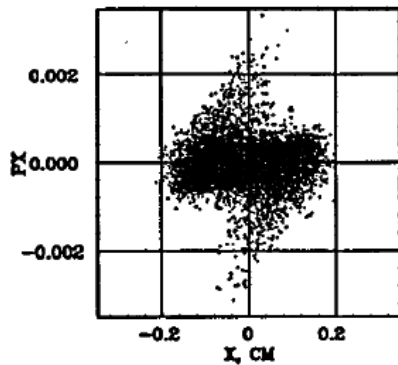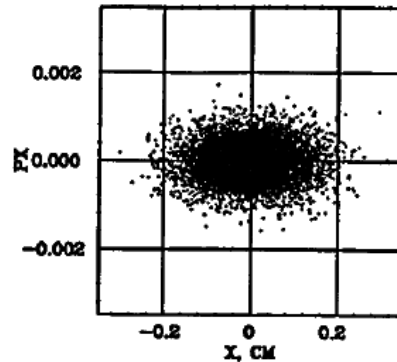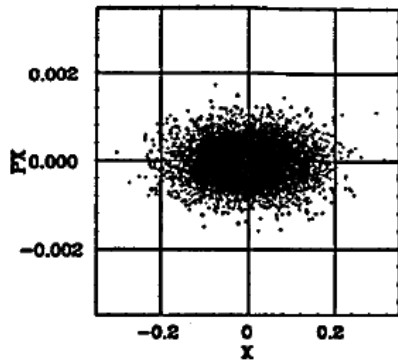
FIG. 6. Emittance growth of the Gaussian beam in the linear focusing channel (upper curve) and emittance conservation in nonlinear focusing channel (lower curve).

FIG. 7. Mismatching of the Gaussian beam in the linear focusing channel (left column) and matching of the same beam with the nonlinear focusing channel (right column).

68

Equilibrium of the beam with "Water Bag" and parabolic distributions

WB distribution in phase space

$$f = f_0, \quad \frac{2}{3}\left(\frac{x^2+y^2}{R^2} + \frac{p_x^2+p_y^2}{p_0^2}\right) \leq 1,$$

$$f = 0, \quad \frac{2}{3}\left(\frac{x^2+y^2}{R^2} + \frac{p_x^2+p_y^2}{p_0^2}\right) > 1.$$

Parabolic distribution in phase space

$$f = f_0\left(1 - \frac{x^2+y^2}{2R^2} - \frac{p_x^2+p_y^2}{2p_0^2}\right)$$

Space charge density

$$\rho(r) = \frac{4I}{3\pi\beta c R^2}\left(1 - \frac{2r^2}{3R^2}\right)$$

Space charge density

$$\rho_b = \frac{3I}{2\pi c \beta R^2}\left(1 - \frac{r^2}{2R^2}\right)^2$$
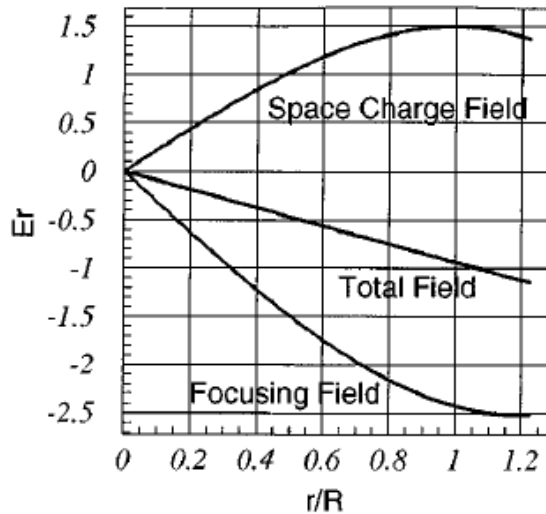
FIG. 4. Total field of the structure E_{tot} [Eq. (12)], required external focusing field E_{ext} [Eq. (21)] and space-charge field E_b [Eq. (20)] of the beam with "water bag" distribution.
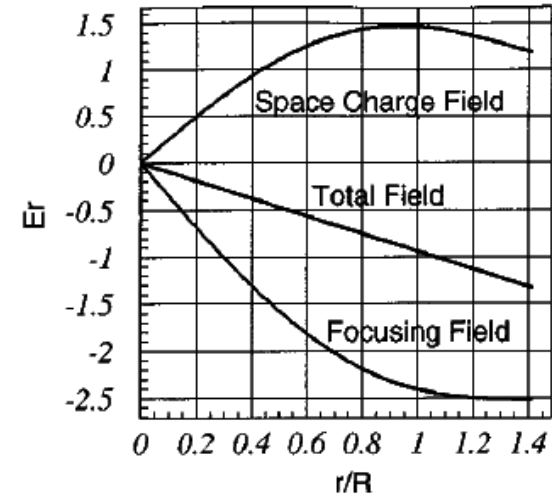
FIG. 5. Total field of the structure E_{tot} [Eq. (12)], required external focusing field E_{ext} [Eq. (25)] and space-charge field E_b [Eq. (24)] of the beam with parabolic distribution.

Focusing by opposite charged particles (plasma lens)

Required potential distribution can be created by introducing inside the transport channel an opposite charged cloud of particles (plasma lens) with the space charge density:

$$\rho_{ext} = \rho_o \, exp(-2\frac{r^2}{R^2}) + \frac{I_c \, \varepsilon^2}{2\pi c \, R^4}$$
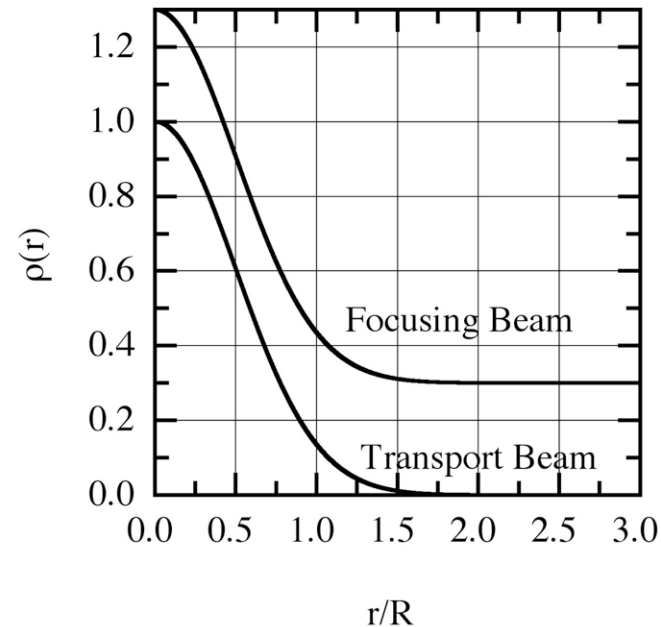
Charged particle density of the transported beam with Gaussian distribution, and of the external focusing beam

Quadrupole-duodecapole focusing structure
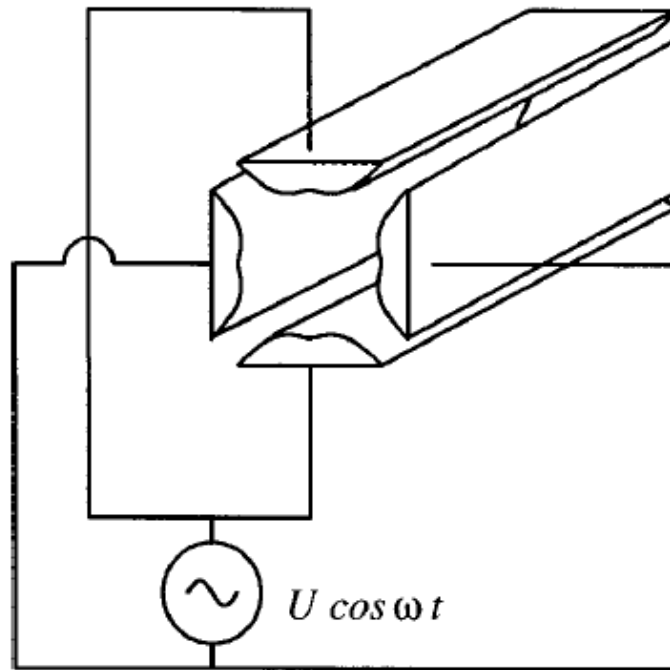
FIG. 6. Proposed four vane quadrupole structure with a duode-
capole field component [5].

Potential of the uniform four vanes structure: $U(r,\varphi,t) = \left(\dfrac{G_2}{2} r^2 \cos 2\varphi + \dfrac{G_6}{6} r^6 \cos 6\varphi \right) \sin \omega_0 t,$

The electrical field of the structure is given by

$$\vec{E}(r,\varphi,t) = [-\vec{i}_r (G_2 r \cos 2\varphi + G_6 r^5 \cos 6\varphi)$$

$$+ \vec{i}_\varphi (G_2 r \sin 2\varphi + G_6 r^5 \sin 6\varphi)] \sin \omega_0 t.$$

an effective scalar potential of the structure [6]

$$U_{ext}(\vec{r}) = \frac{q}{4m\gamma} \frac{E_0^2(\vec{r})}{\omega_0^2}, \tag{6.3}$$

which describes the averaged motion of particle. For the considered structure, the effective potential is

$$U_{ext}(r,\varphi) = \frac{mc^2}{q} \frac{\mu_0^2}{\lambda^2} \left[\frac{1}{2} r^2 + \zeta r^6 \cos 4\varphi + \frac{\zeta^2}{2} r^{10} \right], \tag{6.4}$$

where μ_0 is a smooth transverse oscillation frequency and ζ is a ratio of field components:

$$\mu_0 = \frac{qG_2\lambda^2}{\sqrt{8}\pi mc^2\sqrt{\gamma}}, \quad \zeta = \frac{G_6}{G_2}. \tag{6.5}$$
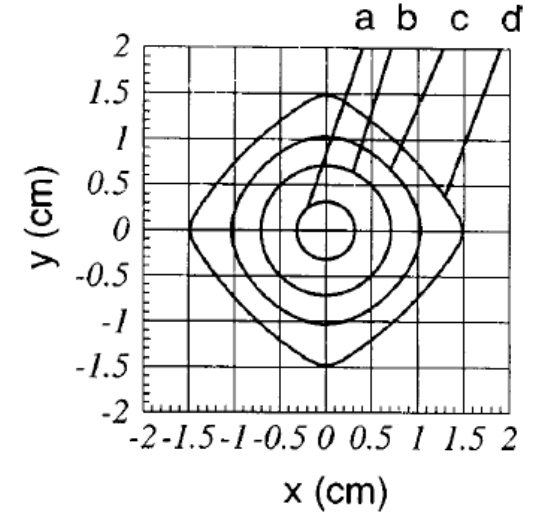
FIG. 7. Lines of equal values of the function $C = \frac{1}{2}r^2 + \zeta r^6 \cos 4\varphi + (\zeta^2/2)r^{10}$ for $\zeta = -0.03$: (a) $C = 0.05$, (b) $C = 0.25$, (c) $C = 0.5$, and (d) $C = 0.85$.

Space-charge density of the matched beam

The space charge distribution of a matched beam can be derived from Poisson's equation via a known space charge potential of the beam

$$\rho_b = -\epsilon_0 \Delta U_b = \frac{\epsilon_0}{1+\delta} \gamma^2 \Delta U_{ext}. \quad (4.26)$$

Application of Eq. (4.26) gives an expression for the self-consistent space charge distribution of the beam in the structure:

$$\rho_b = \rho_0 (1 + 10\zeta r^4 \cos 4\varphi + 25\zeta^2 r^8), \quad (6.6)$$

$$\rho_0 = \frac{2\gamma^2}{(1+\delta)} \frac{mc^2}{q} \frac{\epsilon_0 \mu_0^2}{\lambda^2}. \quad (6.7)$$
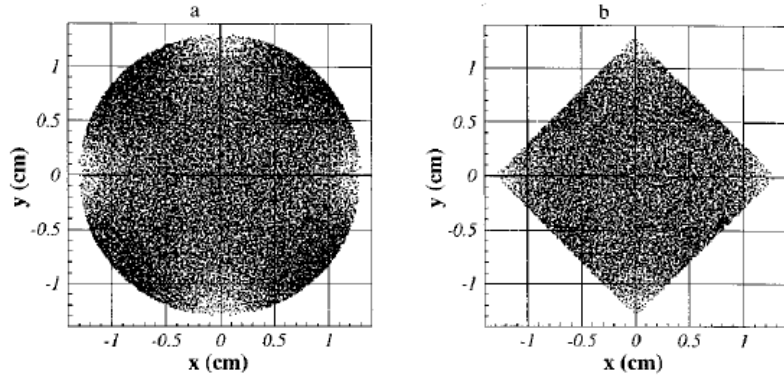
FIG. 8. Self-consistent particle distribution $\rho_b = \rho_0(1 + 10\zeta r^4 \cos 4\varphi + 25\zeta^2 r^8)$ of the matched beam in a quadrupole channel with a duodecapole component with parameter $\zeta = -0.03$: (a) without truncation, (b) with truncation.
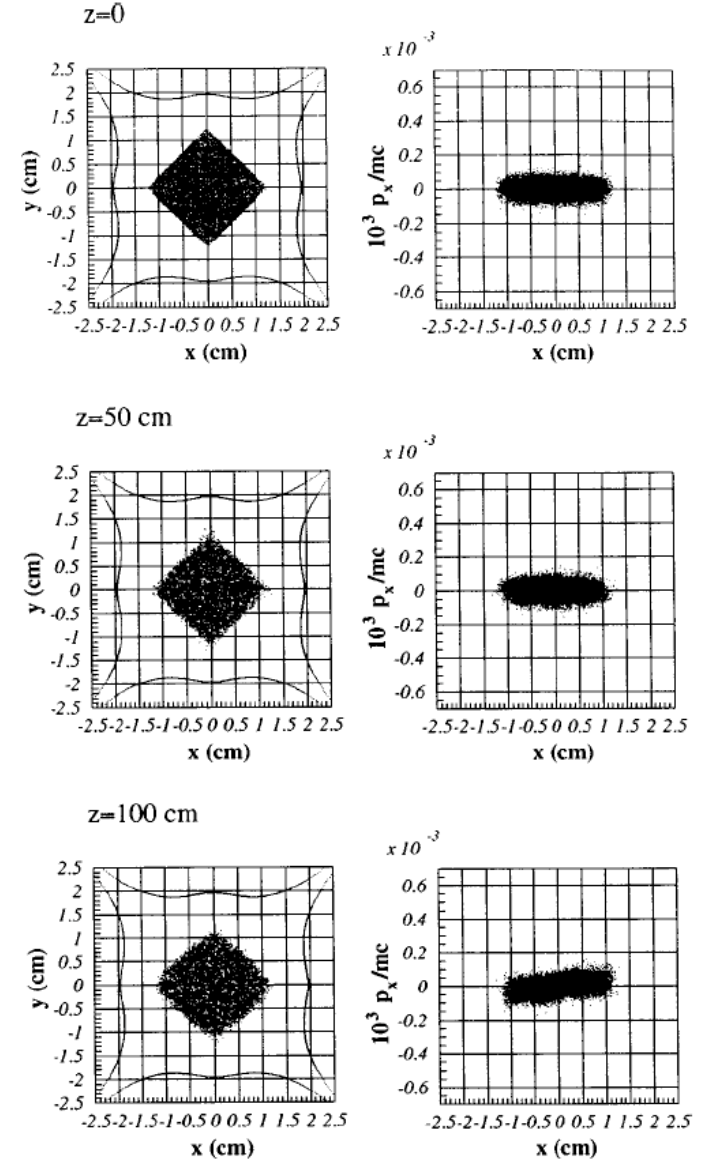
FIG. 9. Emittance conservation of the 150 keV, 100 mA, 0.06π cm mrad proton beam with a matched distribution function (6.14) in a four vane quadrupole structure with field gradient $G_2 = 48$ kV/cm^2 and duodecapole component $G_6 = -1.3$ kV/cm^6.

Proposed FODO Quadrupole - Duodecapole Channel for Suppression of Halo Formation*

Effective potential of quadrupole -duodecapole structure:

$$U_{eff} = (\frac{\mu_o \beta c}{L})^2 [\frac{r^2}{2} + \varsigma r^6 \cos 4\theta + \varsigma^2 \frac{r^{10}}{2}]$$

Quadrupole Gradient–Black   Duodecapole Gradient–Blue

z(cm)
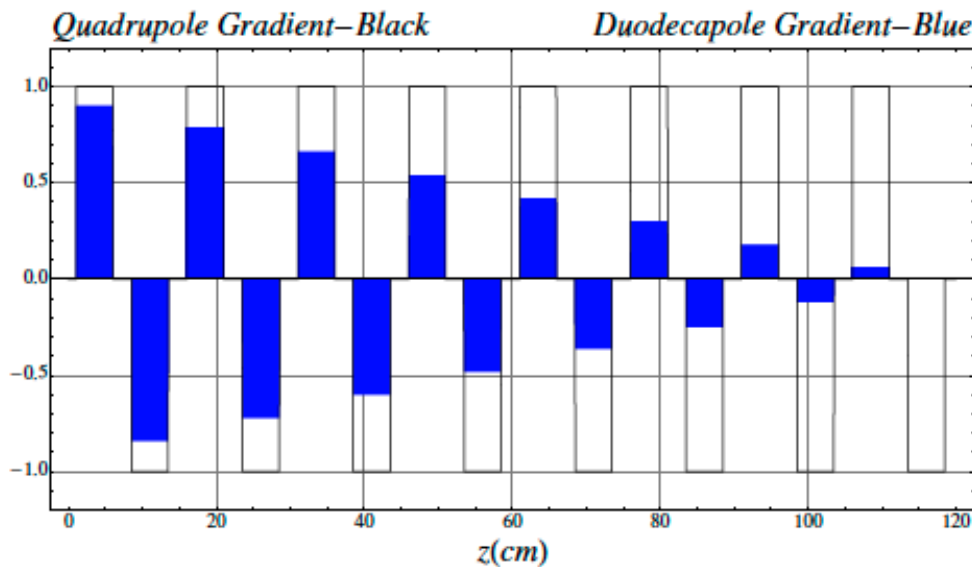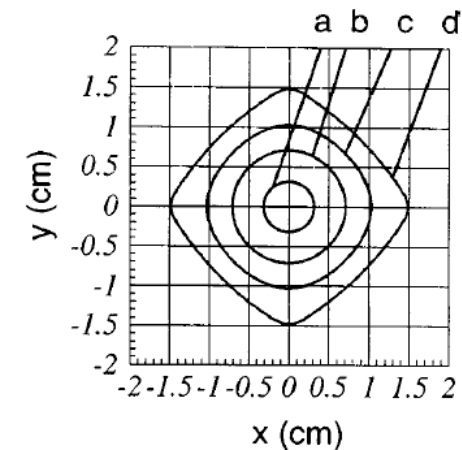
Figure 3: FODO quadrupole-duodecapole channel with combined lenses with the period of $L = 15$ cm, lens length of $D = 5$ cm, and adiabatic decline of duodecapole component to zero over a distance of 7 periods.

Ratio of field components

$$\varsigma = \frac{G_6}{G_2}$$

y (cm)

x (cm)

FIG. 7. Lines of equal values of the function $C = \frac{1}{2} r^2 + \zeta r^6 \cos 4\varphi + (\zeta^2/2) r^{10}$ for $\zeta = -0.03$: (a) $C = 0.05$, (b) $C = 0.25$, (c) $C = 0.5$, and (d) $C = 0.85$.

74

*Y.Batygin, A.Scheinker, WEPPR039, IPAC12

Quadrupole Channel
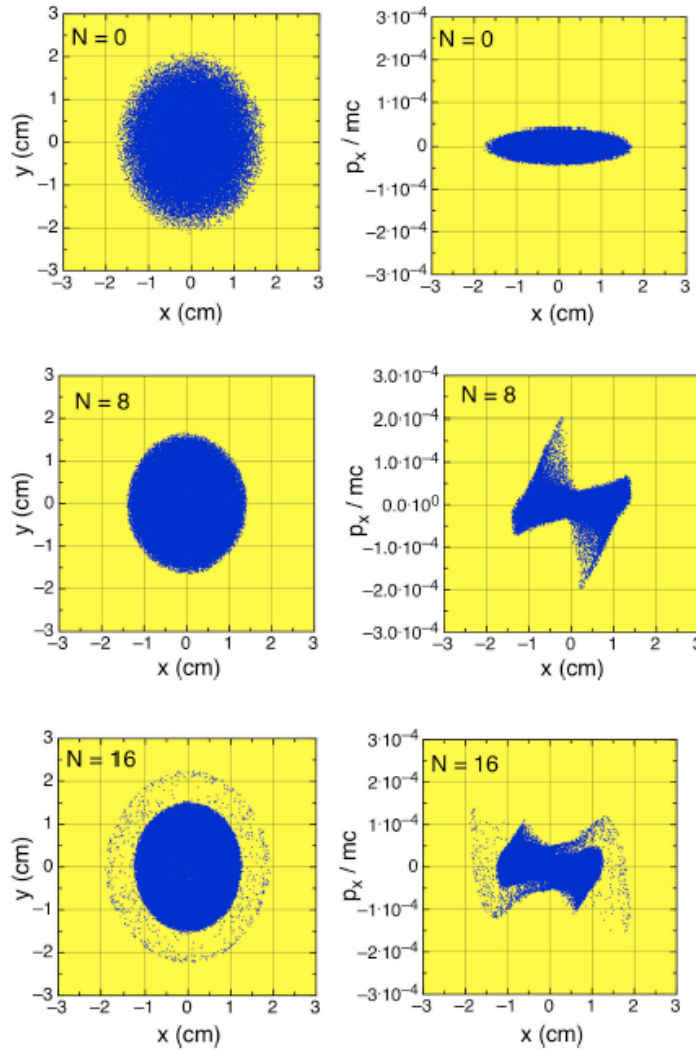
Beam energy	35 keV
Beam current	11.7 mA
Beam emitance	0.05 cm mrad
FODO period	15 cm
Lens length	5 cm
Quadrupole field gradient 0.03579 T/cm	

Quadruple-Duodecapole Channel
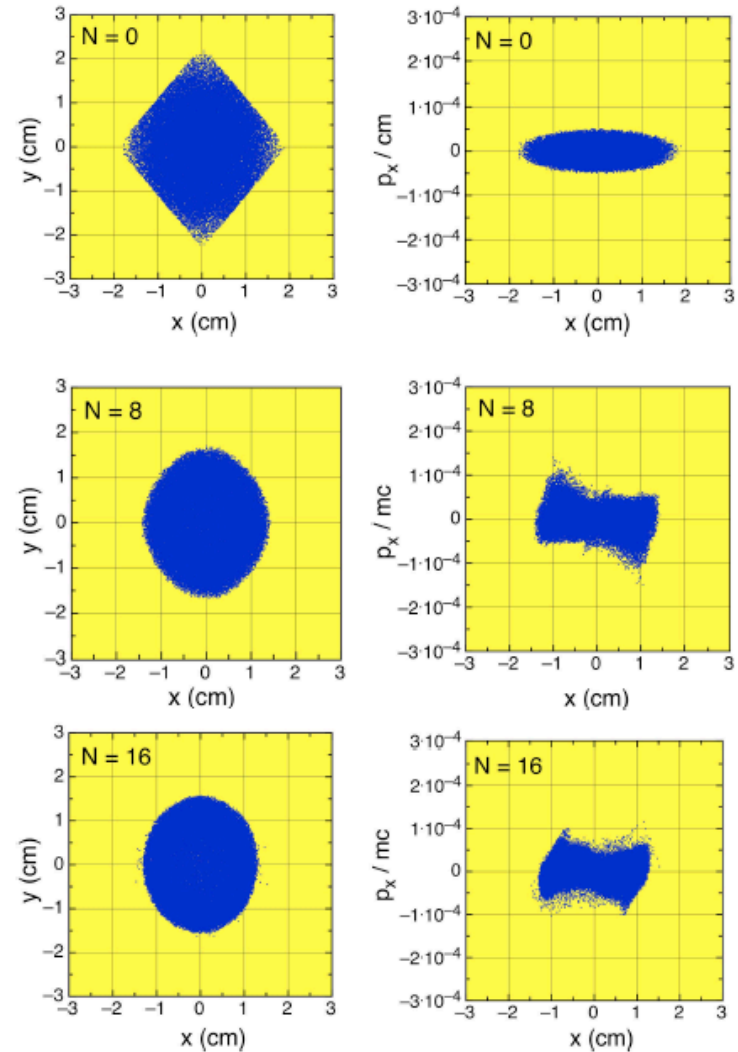
Quadrupole field gradient 0.03579 T/cm
Duodecapole component G_6 = -1.76e-04 T/cm^5
adiabatically decline to zero at the distance of 7 periods.
Numbers indicate FODO periods.

Suppression of Beam Halo
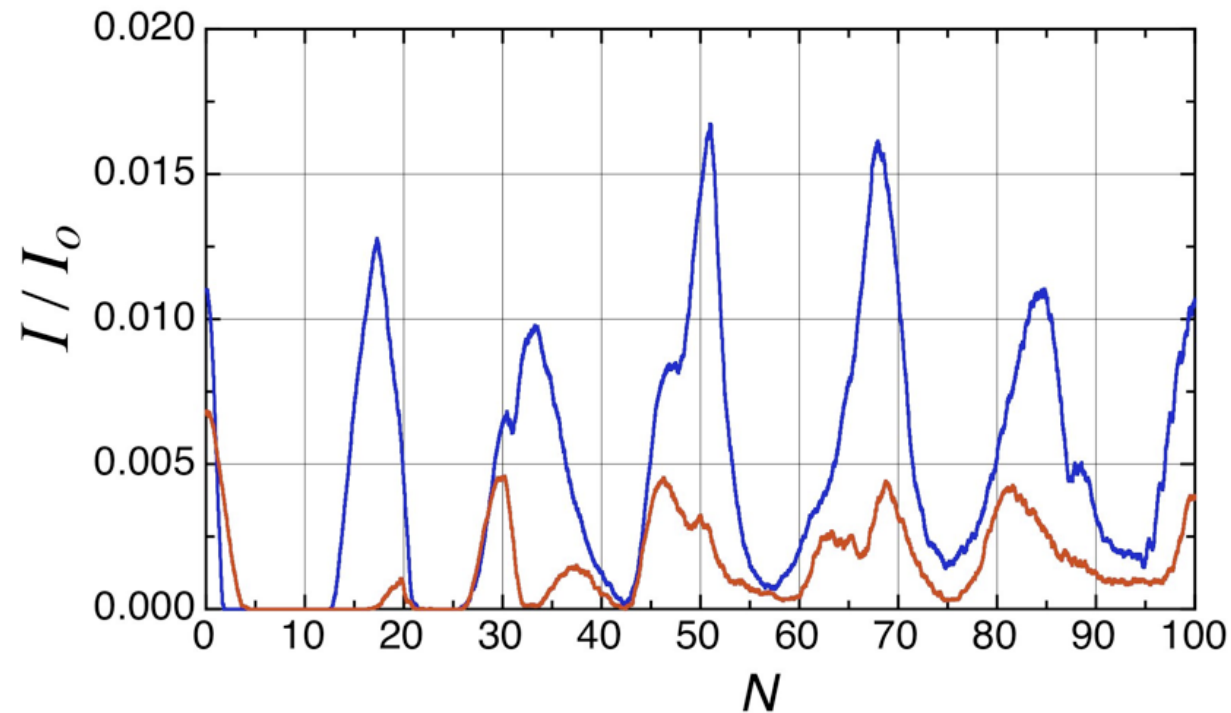
Fraction of particles outside the beam core $2.5\sqrt{<x^2>}$ x $2.5\sqrt{<y^2>}$ as a function of FODO periods: (blue) quadrupole channel, (red) quadrupole-duodecapole channel.

Particle Studio Simulation of Halo Formation in Quadrupole Channel
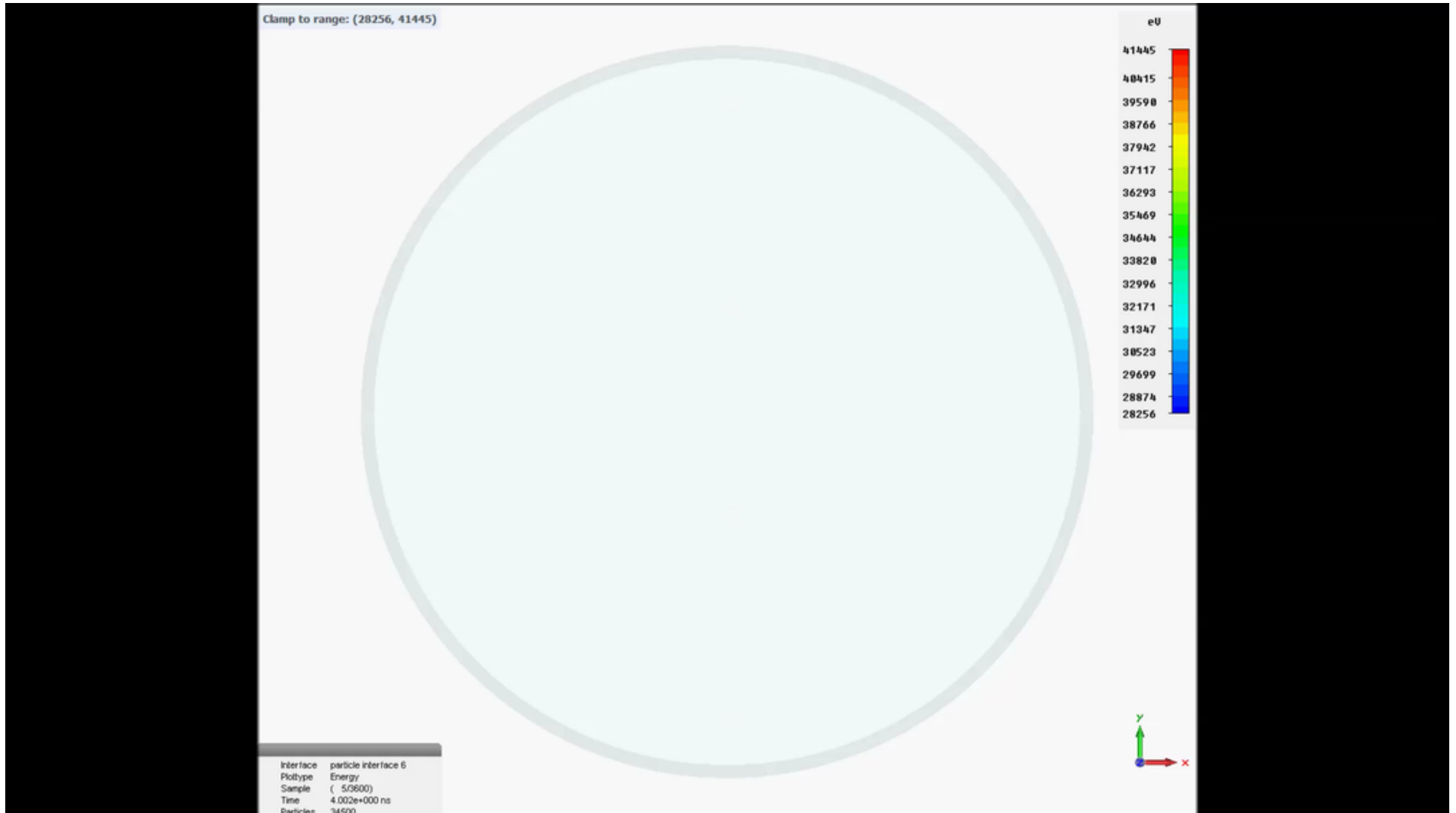
Particle Studio Simulation of Halo Suppression in Quadrupole-Duodecapole Channel
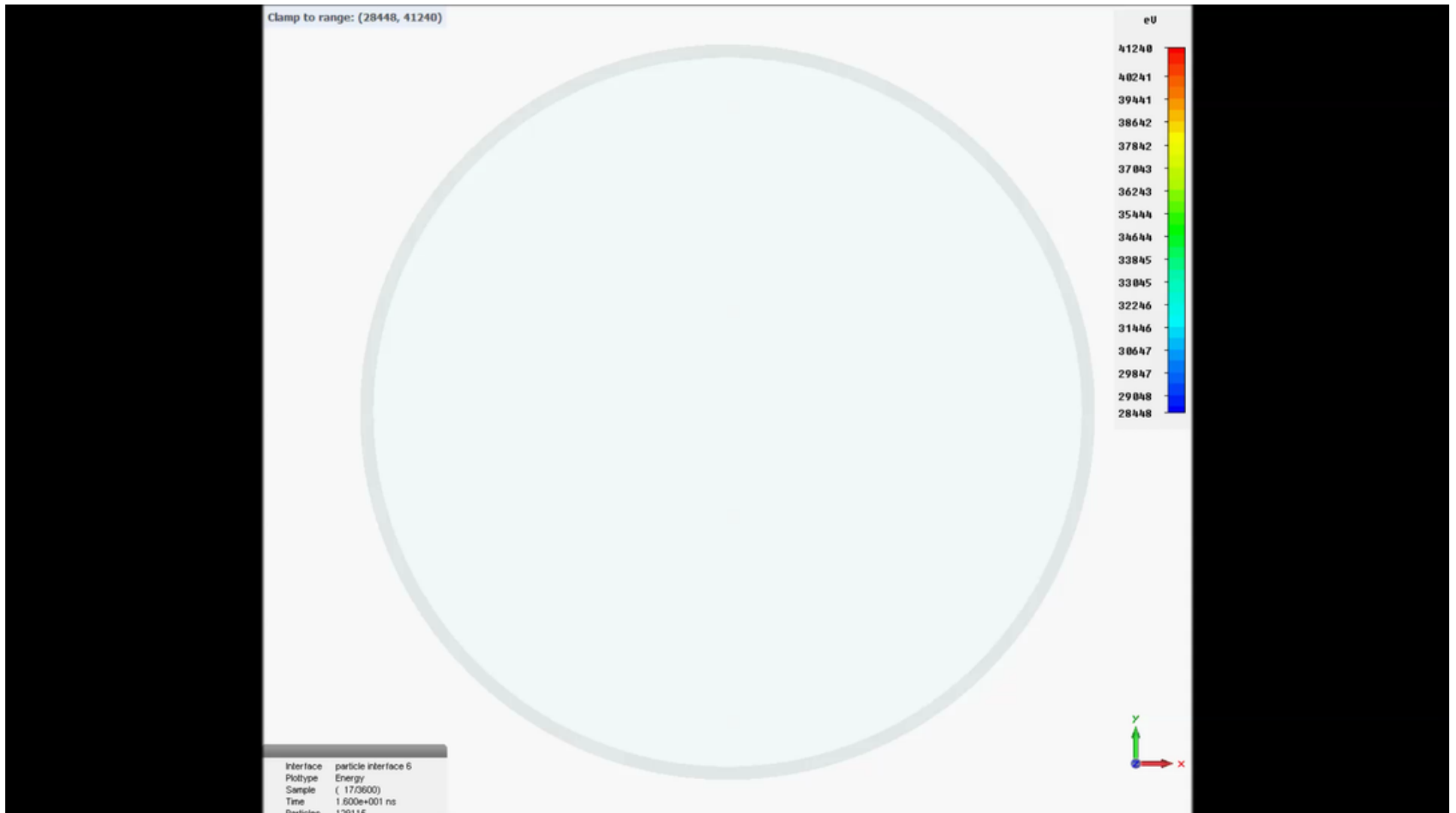
Final Particle Distributions in Focusing Channels

Quadrupole Channel
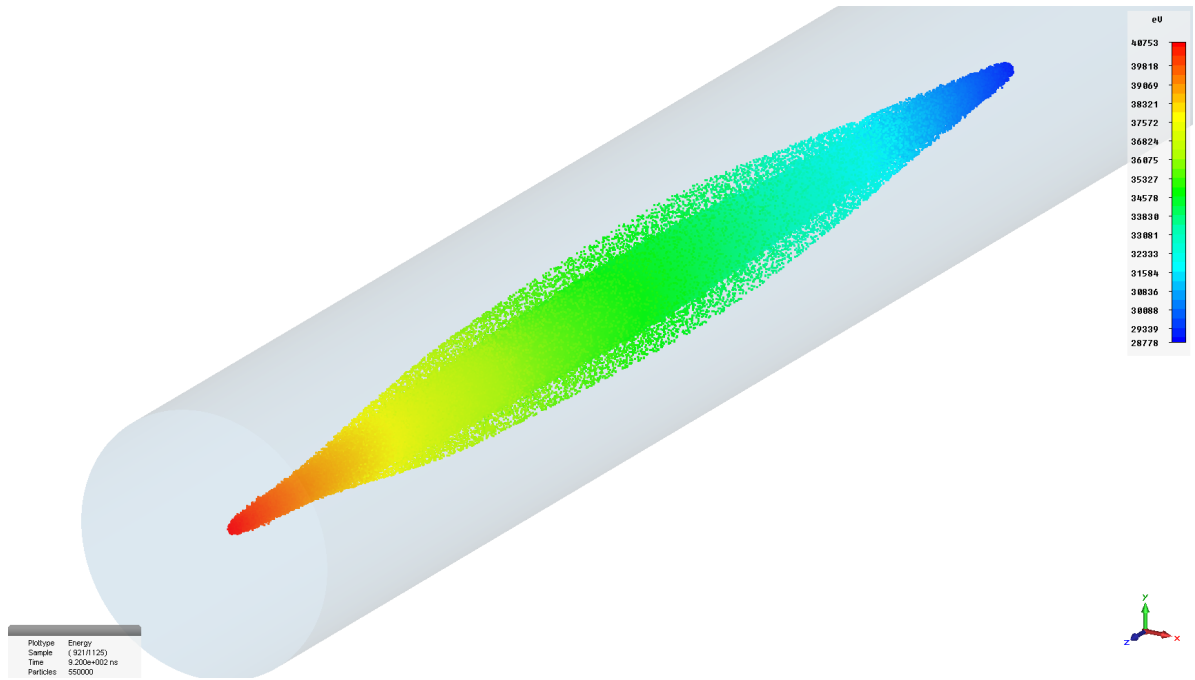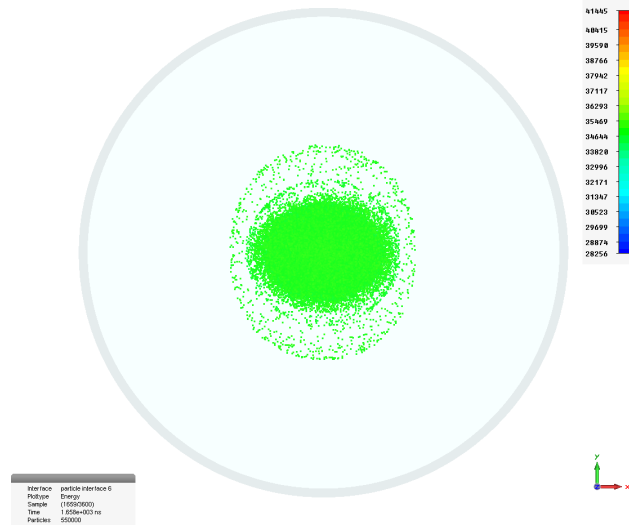
Quadruple-Duodecapole Channel
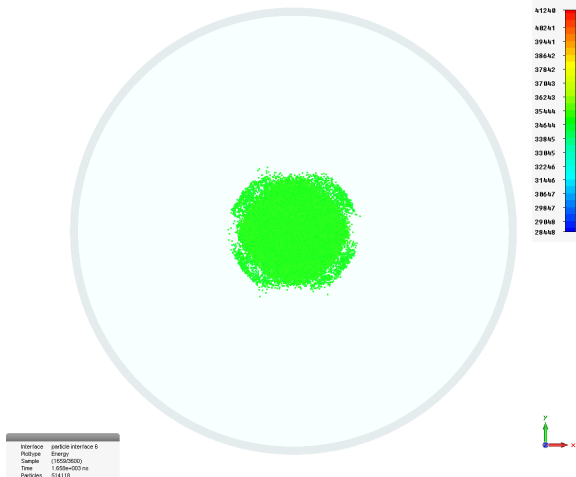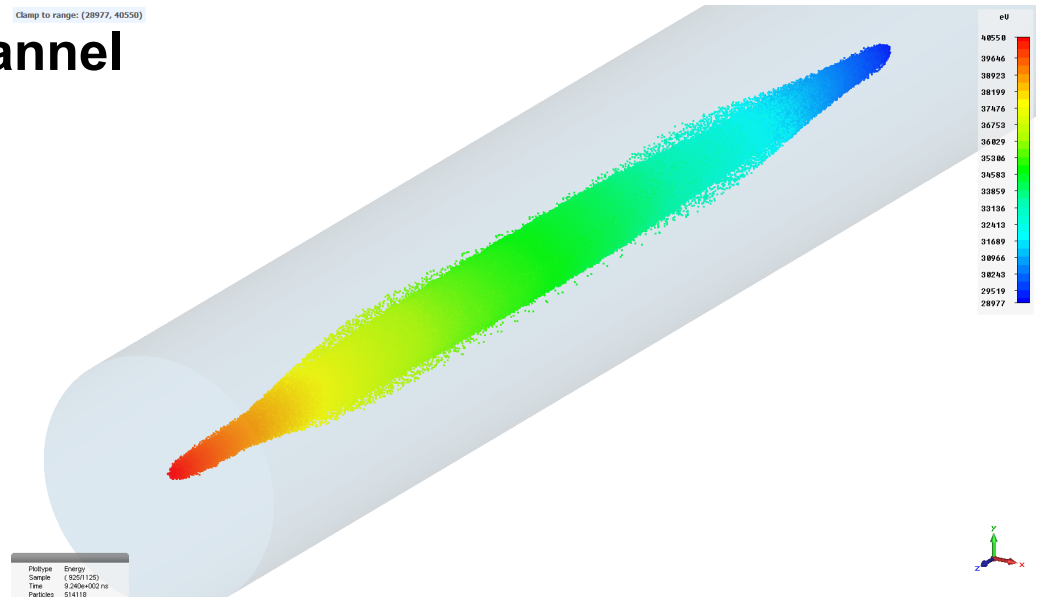
Vibrating Wire Sensor as a Halo Monitor
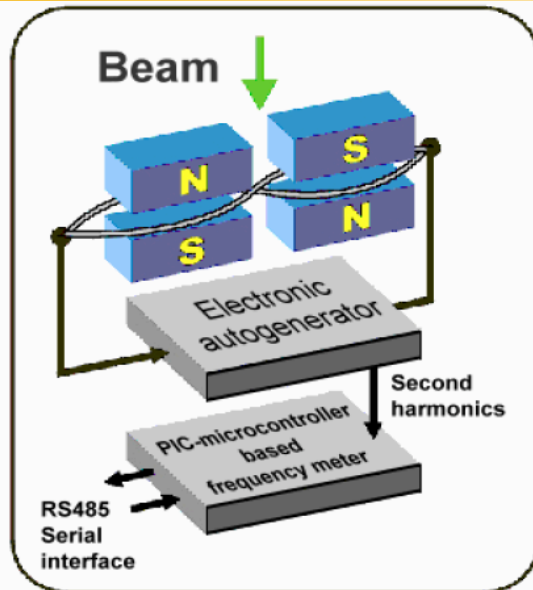
Vibrating wire scanner test in lab
[Arutunian et. al., PAC (March 29 - April 2, 1999, New York City)]

The operating principle of vibrating wire sensors is measurement of the change in the frequency of a vibrating wire, which is stretched on a support, depending on the physical parameters of the wire and the environment in

By use of a simple positive feedback circuit, the magnetic system excites the second harmonic of the wire's natural oscillation frequency while keeping the middle of the wire exposed for detection of beam heating.

The interaction of the beam with the wire mainly causes heating of the wire due to the energy loss of the particles

Scan of the electron beam at the Injector of Yerevan Synchrotron with an average current of about 10 nA (after collimation) and an electron energy of 50 MeV

80